



**FACULTY
OF MATHEMATICS
AND PHYSICS**
Charles University

MASTER THESIS

Andrej Liška

**The cosmological constant on the
non-cosmological scales**

Astronomical Institute of the Charles University in Prague

Supervisor of the master thesis: doc. RNDr. Attila Mészáros, DrSc.

Study programme: Physics

Study branch: Astronomy and Astrophysics

Prague 2021

I declare that I carried out this master thesis independently, and only with the cited sources, literature and other professional sources. It has not been used to obtain another or the same degree.

I understand that my work relates to the rights and obligations under the Act No. 121/2000 Sb., the Copyright Act, as amended, in particular the fact that the Charles University has the right to conclude a license agreement on the use of this work as a school work pursuant to Section 60 subsection 1 of the Copyright Act.

In date
Author's signature

First of all, I would like to thank my supervisor doc. RNDr. Attila Mészáros, DrSc., for his advice, expertise, time spent in consultations and overall guidance. My thanks goes to my family Lýdia, Štefan and Frederik for their support in studying and creating suitable working conditions, either during the exam period or in writing this master thesis. Last but not least, many thanks to Michaela Stronerová for the peace and support she provided me at the time of writing. In conclusion, I thank my colleagues Marcel Štolc and Michal Kyjovský for their help and constant encouragement.

Many thanks to everyone.

Title: The cosmological constant on the non-cosmological scales

Author: Andrej Liška

Department: Astronomical Institute of the Charles University in Prague

Supervisor: doc. RNDr. Attila Mészáros, DrSc., Astronomical Institute of the Charles University in Prague

Abstract: The cosmological constant Λ was first added to the gravitational field equations in 1917 by Albert Einstein. Einstein preferred the static universe, whereas field equations without the cosmological constant did not allow for such a scenario. A series of later observations mainly by Slipher, Lemaître and Hubble showed the universe to be dynamic, which led to the cosmological constant being neglected from Einstein's field equations. In the early 1990s, it became clear that the expansion of the universe accelerates and the cosmological constant emerged in the field equations again, as an explanatory element. Based on a study by Perlmutter and Riess who observed distant type Ia supernovae, the cosmological constant is positive with a value of 10^{-56} cm^{-2} . The 2011 Nobel Prize was awarded for this discovery. Within the limit of weak gravitational fields and low velocities, Einstein's theory of gravitation must be reduced into Newtonian theory of gravity, the so-called Newtonian limit of Einstein equations. The full Einstein equations of the gravitational field, in the Newtonian limit, are not reduced exactly to Poisson's equation of Newtonian theory of the gravitational field. The Newtonian limit contains two additional terms with the cosmological constant, which the classical theory of gravity does not account for. The potential difference between the Poisson equation and the Newtonian limit must be at non-cosmological distances (typical distances of the solar system) negligible. The numerical solution of the given potentials shows changes in the differences with respect to the choice of density profiles.

Keywords: General theory of relativity, cosmological constant, observational data, astronomical distances

Název práce: Kosmologická konstanta na nekosmologických škálách

Autor: Andrej Liška

Department: Astronomický ústav Univerzity Karlovy v Praze

Vedoucí diplomové práce: doc. RNDr. Attila Mészáros, DrSc., Astronomický ústav Univerzity Karlovy v Praze

Abstrakt: Kosmologická konstanta Λ byla poprvé přidána do rovnic gravitačního pole v roce 1917 Albertem Einsteinem. Einstein preferoval statický vesmír, což polní rovnice bez kosmologické konstanty neumožňovaly. Série pozdějších pozorování hlavně Sliphera, Lemaître a Hubblea ukázala dynamičnost vesmíru, což vedlo od upuštění kosmologické konstanty z Einsteinových polních rovnic. Začátkem 90. let se ukázalo, že rozpínání vesmíru akceleruje, čímž byla kosmologická konstanta opět dosazena do polních rovnic jako vysvětlující element. Na základně studie Perlmuttera a Riessa, kteří pozorovali vzdálené supernovy typu Ia, je kosmologická konstanta kladná z hodnotou 10^{-56} cm^{-2} . Za tento objev byla udělena v roce 2011 Nobelova cena. V limitě pro slabé gravitační pole a malé rychlosti se musí einsteinova teorie gravitace redukovat v Newtonovskou teorii gravitace, tzv. Newtonovskou limitu Einsteinových rovnic. Plné Einsteinovy rovnice gravitačního pole se v Newtonovské limitě neredukují přesně na Poissonovu rovnici Newtonovské teorie gravitačního pole. Newtonovská limita obsahuje navíc dva členy s kosmologickou konstantou, které klasická teorie gravitace nezná. Rozdíl potenciálů Poissonovy rovnice a Newtonovské limity musí být na nekosmologických vzdálenostech (typické vzdálenosti pro sluneční soustavu) zanedbatelný. Numerické řešení daných potenciálů vykazuje změny v rozdílech vzhledem k volbě hustotních profilů.

Klíčová slova: Obecná teorie relativity, kosmologická konstanta, observační data, astronomické vzdálenosti

Contents

Introduction	2
1 Development of cosmological constant Λ	4
2 Introduction and existence of cosmological constant Λ	6
2.1 The existence of cosmological constant Λ	6
2.2 Intuitive meaning of cosmological constant	8
2.2.1 Cosmological constant Λ as a source	8
2.2.2 Cosmological constant Λ as an independent constant of Einstein's equations	9
3 Newtonian limit	10
3.1 Newtonian limit without cosmological constant	10
3.2 Newtonian limit with cosmological constant	13
4 Solution of the Newtonian limit	16
4.1 Numerical solution in Cartesian coordinates	16
4.2 Numerical solution in Spherical coordinates	18
4.3 Numerical solution in Polar coordinates	22
5 Results	26
5.1 Sun-Jupiter distance	28
5.2 Sun-Voyager I distance	33
5.3 Distance of the gravitational interaction of the sun	38
5.4 Distance of the radius of our galaxy	43
5.5 Commentary on the numerical solutions	48
Conclusion and future perspectives	49
Bibliography	50
List of Figures	53
List of Tables	55
List of Abbreviations	56
A Analytical solution and Taylor series	57
A.1 Analytical solution of the Newtonian limit for vacuum	57
A.2 Taylor series of the vacuum solution	60

Introduction

In 1917, Albert Einstein added the cosmological term $\Lambda g_{\mu\nu}$ to his equations of the gravitational field. Einstein assumed the existence of a static universe, which, however, was not a solution to his originally published field equations in 1915. Stationarity was achieved by the just-introduced additional term proportional to the metric tensor. The cosmological constant, which was thus added to Einstein's field equations at the time, lead to a solution for the static universe.

Extensive observations in the 1920s and 1930s have shown that the universe is probably not static, as Einstein predicted. It was mostly the work of Slipher, Lemur, Robertson and Hubble that brought a non-trivial relationship between redshift and distance, i.e. the correlation between the radial velocity and the distance of an object. This dependence showed that the universe must expand, hence it is dynamic. Einstein therefore abandoned the static universe and excluded the cosmological constant from the field equations. In 1917 he described its introduction as *the biggest blunder* of his life.

New research and observations, mainly under the leadership of Perlmutter and Riess, again point to a cosmological term. Due to the observation of distant supernovae, it has been shown that the universe is not only expanding, but the expansion itself is accelerating. This discovery again introduced the cosmological constant into Einstein's equations of the gravitational field, as a term explaining this accelerated expansion. The cosmological constant plays the role of so-called dark energy. In 2011, Saul Perlmutter, Adam Riess and Brian P. Schmidt were awarded the Nobel Prize for the discovery of the accelerating expansion of the universe.

Assuming the validity of the basic principles of the general theory of relativity, the cosmological term automatically appears on the left-hand side side of the Einstein equations. If, however, Einstein's theory of gravitation is to be an extension of Newton's theory of gravity, then for low velocities and weak gravitational fields, Einstein's theory must give the same results as Newton's theory. We call this limit case the Newtonian limit of Einstein's equations.

The inconsistency of the Newtonian limit lies precisely in the cosmological constant, which does not appear in the classical theory of gravity. Unlike the Poisson equation for Newtonian theory, the Newtonian limit has 2 terms with the cosmological constant. These terms cause a difference in the resulting potentials. In order for the classical Newtonian theory of gravity to remain valid, it is necessary to arrive at insignificant differences on small scales in the solar system, where the classical Newtonian theory gives reliable results.

The aim is to show how these differences will change on small distances (characteristic distances of the solar system - of the order of the astronomical unit) for different density profiles. We further discuss whether today's instruments can observe such deviations and thus determine the cosmological constant on small

scales. We also discuss the significance of the modified Poisson equation considering greater distances (galactic scales in light years) for different density profiles.

1. Development of cosmological constant Λ

The cosmological constant Λ is one of the constituents present in Einstein equations (hereafter EE). Especially, it is part of the left "geometric" side. However, Einstein published his equations of the gravitational field in the 25-th of November 1915 in Berlin [Einstein, 1915] primarily neglecting the cosmological constant.

The equations read as

$$G_{im} = -\kappa(T_{im} - \frac{1}{2}g_{im}T). \quad (1.1)$$

From eq. (1.1), we see that Einstein denoted the indices by the classical Latin alphabet (i, m, \dots), while throughout the text we will use Greek letters (α, β, \dots) to denote the indices of tensors.

The field equations defined in this way do not support the closed static universe, which according to Einstein corresponds precisely to the model supported by nature. In 1917, he added the Λ -term to account for the static universe. In the following Chapters we will show that we get the Λ -term into EE starting from the basic principles of the general theory of relativity, i.e. without requiring the universe to be static or dynamic. The equations of the gravitational field he published in 1917 are as follows [Einstein, 1917]

$$G_{\mu\nu} - \Lambda g_{\mu\nu} = -\kappa \left(T_{\mu\nu} - \frac{1}{2}g_{\mu\nu}T \right). \quad (1.2)$$

In 1922, Friedmann solved EE for a homogeneous and isotropic universe. The keystone of these models is the so-called FRLW metrics. Friedman's equations were derived based on the full EE (1.2) and therefore contained the Λ -term. By default, Friedmann formulated only one equation. However, two are commonly used. The second one is derived from the first and also contains the cosmological term Λ [Friedmann, 1922].

Despite his belief in the closed, static universe, Einstein set the cosmological constant in Friedman's equations to zero, thus obtaining a homogeneous and isotropic solution. The solution was the expanding universe known today as the Friedmann-Einstein universe [Einstein, 2006].

In the following years, it really turned out that nature supports a dynamic universe rather than a static one. The dynamically expanding universe was mainly supported by Lemaître, Slipher and Hubble. They showed a linear correlation between the red shift, i.e. the speed of the object's distance and its distance from the observer. Observational data then clearly contradicted the theory of the static universe [Slipher, 1917, Lemaître, 1927, Hubble, 1929]. Einstein therefore again excluded the cosmological term $\Lambda g_{\mu\nu}$ from his equations and declared that the introduction of this term into gravitational field equations was *the biggest*

blunder in his life¹. It is possible that Gamow paraphrased this statement in his biography in his own way [Gamow, 1956].

Since the late 1930s, a number of astronomers have taken the cosmological term in the field equations as redundant. When solving problems, the cosmological constant was automatically assumed to be zero. This state lasted until the 1990s, with the exception of the 1950s, when the cosmological constant appeared for some time in poly-particle physics [Weinberg, 1989, Carroll et al., 1992].

At the beginning of the third millennium, observations of distant type Ia². Several teams, mainly around Perlmutter and Riess, have studied the significance of the cosmological term on supernovae Ia, which show a significant redshift. The results of the measurements clearly point to an accelerating universe that is expanding. The gravity resulting from visible matter is not enough to hold it together, which necessarily implies the non-zero character of the cosmological constant Λ . This significant discovery contributed to the re-introduction of the cosmological term with the cosmological constant into EE. In 2011, the discovery of the accelerating expansion of the universe was awarded the Nobel Prize for Saul Perlmutter, Adam Riess and Brian P. Schmidt. Today, this model of the universe is known as the standard model [Perlmutter et al., 1999, Riess et al., 1998].

In cosmology, instead of the Λ -term itself, the ratio between the energy density caused by the cosmological constant and the critical density of the universe is often used, denoted as Ω_Λ . Recent research points to the significance of this term, which is approximately equal to $\Omega_\Lambda \approx 0,7$ [Baker et al., 1999]. Let us realize that today's standard model of the universe includes more than a third of all energy, the so-called dark energy, which acts against gravity.

The most recent measurements of the cosmological constant in the universe set its value at 10^{-56} cm^{-2} [Kohn, 2020]. The quantum field theory contradicts this value and predicts a huge value for the quantum vacuum. The quantum vacuum defined in this way is equivalent to the cosmological constant, which means that the values should be the same. However, the results predicted by the quantum field theory differ by about 120 orders of magnitude compared to the measured cosmological constant. This is the greatest discrepancy between the theoretical prediction and the actual measured value in the history of physics [Rugh and Zinkernagel, 2002, Adler et al., 1995].

¹Recent research shows that Einstein may never have made the notorious statement *the biggest blunder* [Livio, 2013].

²Supernovae of this type are exceptionally bright standard candles, with which it is possible to reliably calculate the distance from the observer with respect to the observed luminosity. Before 90's, it was difficult to discover these supernovae in galaxies due to a lack of technology. Projects led by Perlmutter and Riess already had larger telescopes at their disposal, with which it was possible to detect the given types and thus study them, which enabled the mentioned discovery [Perlmutter et al., 1998].

2. Introduction and existence of cosmological constant Λ

Next we will work with the following notation. Any other cases or changes in notation will be explicitly mentioned.

- The time component will be negative, while the spatial components will be positive. We will therefore work with the signature $(-1,1,1,1)$. However, Einstein relied on the inverse signature, i.e. $(1,-1,-1,-1)$ (see eq. (1.2)).
- We will consider geometrized units, where the gravitational constant G and the speed of light c are equal to one. For consistency, the essential formulas will also be given in standard units.

We will show that the existence of cosmological constant Λ stems directly from the basic principles of the general theory of relativity and the significance of the quantities that characterize this theory. The full EE of the gravitational field will clearly define the cosmological term with Λ .

2.1 The existence of cosmological constant Λ

EE, like Maxwell's equations, are fundamental, in other words, they are not derived from other equations. They are deductively derived from the developed theory of the gravitational field based on the initial principles that must apply to the theory.

The only way to work on EE is to use the existing theory of the gravitational field, i.e. Newton's theory, and transform it into Einstein's. Newton's theory is characterized by the Poisson equation, i.e.

$$\Delta\phi(t, \vec{r}) = 4\pi\rho(t, \vec{r}), \quad (2.1)$$

where the gravitational constant G is assumed to be equal to 1, given that we consider geometrized units. In standard units, the eq. (2.1) reads as $\Delta\phi(t, \vec{r}) = 4\pi G\rho(t, \vec{r})$.

The eq. (2.1) contains several problems which, when solved, lead to EE. First of all, it is good to realize that the given eq. (2.1) describes the effect immediately. Both the potential ϕ and the density ρ depend on time and the position vector \vec{r} , while the time is exactly the same on both sides. On the right side there is no retardation of time. There is no propagation between bodies in finite time, but infinite instead. Thus, if the field is to propagate the eq. (2.1) should contain not only spatial derivatives, but also a temporal derivative, which does not occur there. This discrepancy is at odds with causality.

The second problem that the eq. (2.1) poses is that it is not covariant. Because if it met the principle of general covariance, it would have to be invariant. The left side of the Poisson equation is invariant, which can be seen by replacing

the Laplace operator Δ with the d'Alambert operator \square , solving the first causality problem, as d'Alambert also contains the second time derivative¹. However, the right-hand side of the eq. (2.1) is not an invariant because the density of ρ in Newtonian theory of gravity is given by the relation $\frac{dM}{dV}$, where dM is not the rest mass and dV is not the rest volume. This problem can also be solved if we write ρ_0 , i.e. the proper density, instead of ρ . Thus we re-write the eq. (2.1) to the tensorial form, which already satisfies the condition of causality and also the condition of general covariance.

$$\phi^\mu_{;\mu} = 4\pi\rho_0. \quad (2.2)$$

The newly formed eq. (2.2) is valid only in the rest system, because only in such a system can the gravitational action of a substance be described by the rest density ρ_0 . In the general theory of relativity, we need the field equations to be valid not only in a rest system, but in any system. We replace the right side of the eq. (2.2) with the energy and momentum tensor $T^{\mu\nu}$, which captures not only the energy density, but also the energy density flow and the momentum density flow, necessary to describe the gravitational interaction in the general system.

On the left side, in the original Poisson eq. (2.1), the Laplace operator appears. This operator is linear in second derivatives and in the Chapter 3, we show that the equivalent quantity against the potential *phi* in the general theory of relativity is the metric, i.e. the components of the metric tensor $g_{\mu\nu}$. Thus, it is natural to require that the left side contain a second-order tensor, since the right side is proportional to $T^{\mu\nu}$. Another requirement for the left side is that it must contain metric, its first derivatives and its second derivatives. Derivatives of higher order of the metric can be neglected due to the fact that the Laplace operator is second order and we also require that the second derivatives of the metric to be linear, which again follows from the nature of the Laplace operator. Let us define the left side as

$$A_{\mu\nu} = A_{\mu\nu}(g_{\alpha\beta}, g_{\alpha\beta,\gamma}, g_{\alpha\beta,\gamma\delta}). \quad (2.3)$$

It will be clear from the forthcoming Chapters that the first derivatives of the metric are clearly connected with Christoffel's symbols. The problem is that Christoffel symbols are not tensors because they can be reset in a locally inertial system. However, we will require that the dependence of the searched left side does not depend on the system in which we are, so we no longer have to directly consider the first derivatives of the metric in the searched form of the tensor $A_{\mu\nu}$.

It can be shown that every tensor $A_{\mu\nu}$ defined in this way can be expressed unambiguously using the variables g_β and $R_{\alpha\beta\gamma\delta}$, i.e. using both metrics and Riemann's tensor, which must be linear. This restriction reduces the tensor $A_{\mu\nu}$ to

$$A_{\mu\nu} = A_{\mu\nu}(R_{\mu\nu}, Rg_{\mu\nu}, g_{\mu\nu}). \quad (2.4)$$

The dependence of the individual variables in the rule for $A_{\mu\nu}$ will define the left side of EE. We will rewrite the original equations of the gravitational field (2.1)

¹In the equation: $\square\phi \equiv \phi^\mu_{;\mu} \equiv g^{\mu\nu}\phi_{;\mu\nu}$, is ϕ invariant, then the whole left side of the eq. (2.1) is invariant.

in the form

$$c_1 R_{\mu\nu} + c_2 R g_{\mu\nu} + c_3 g_{\mu\nu} = c_4 T_{\mu\nu}. \quad (2.5)$$

It is possible to derive the relationship between the constants c_1 and c_2 if we use the 2-nd Bianchi identity in the following form

$$R^{\mu\nu}{}_{[\alpha\beta;\rho]} = 0 \quad (2.6)$$

and conservation laws

$$T^{\mu\nu}{}_{;\nu} = 0. \quad (2.7)$$

The final form of the coefficients that multiply the terms in EE by $R_{\mu\nu}$, $Rg_{\mu\nu}$, $g_{\mu\nu}$ and $T_{\mu\nu}$ are 1 , $-\frac{1}{2}$, $\frac{c_3}{c_1}$ and $\frac{c_4}{c_1}$, respectively.

The left side of EE represents the geometry of space-time. In addition to the contraction of the Riemann tensor, the metric tensor multiplied by the constant $\frac{c_3}{c_1}$, which we denote as Λ , enters the geometry of space-time as well. We have shown that the full EE of the gravitational field necessarily contain a Λ -term, which is also called a cosmological term.

2.2 Intuitive meaning of cosmological constant

The source right hand-side of EE contains the energy and momentum tensor $T_{\mu\nu}$. This tensor can be defined for different media. In our applications, we will further use its prescription for charged incoherent dust and for an ideal fluid. So let's define the energy and momentum tensor for charged incoherent dust as

$$T_{\mu\nu}^{dust} = g_{\alpha\mu} g_{\beta\nu} \rho u^\alpha u^\beta \quad (2.8)$$

and for an ideal fluid as

$$T_{\mu\nu}^{fluid} = g_{\alpha\mu} g_{\beta\nu} [(\rho + P)u^\alpha u^\beta + P g^{\alpha\beta}]. \quad (2.9)$$

2.2.1 Cosmological constant Λ as a source

Let's define EE for an ideal fluid as

$$R_{\mu\nu} - \frac{1}{2} R g_{\mu\nu} + \Lambda g_{\mu\nu} = 8\pi [(\rho + P)u_\mu u_\nu + P g_{\mu\nu}]. \quad (2.10)$$

The energy-momentum tensor of an ideal fluid has, in contrast to the energy-momentum tensor of dust, an additional component – pressure. Thus, the difference lies within the interaction being involved in the equations of its components via pressure, whereas in the case of the energy-momentum tensor of dust there is no such a term.

Let's re-arrange the eq. (2.10) to better understand the meaning of the Λ -term.

$$\begin{aligned} R_{\mu\nu} - \frac{1}{2} R g_{\mu\nu} &= 8\pi [(\rho + P)u_\mu u_\nu + P g_{\mu\nu}] - \Lambda g_{\mu\nu} \\ &= 8\pi [(\rho + P)u_\mu u_\nu] + (8\pi P - \Lambda)g_{\mu\nu}. \end{aligned} \quad (2.11)$$

Note from eq. (2.11) that Λ -term in EE is acting against pressure. We know from Euler's equations that pressure acts similarly to the density of matter, from which we can directly characterize the significance of the negative and positive value of the cosmological constant. For $\Lambda > 0$ with respect to what is written, we can state that it acts repulsively, unlike $\Lambda < 0$, which acts attractively.

To further clarify the Λ -term in EE let's assume the vacuum system, i.e. $T_{\mu\nu} = 0$

$$R_{\mu\nu} - \frac{1}{2}Rg_{\mu\nu} + \Lambda g_{\mu\nu} = 0. \quad (2.12)$$

Let's place the term with the Λ ($\Lambda g_{\mu\nu}$) to the right-hand side and notice that it acts as source, i.e.

$$R_{\mu\nu} - \frac{1}{2}Rg_{\mu\nu} = -\Lambda g_{\mu\nu}. \quad (2.13)$$

Comparing the eq. (2.13) to the expression of the energy-momentum tensor of an ideal fluid given by (2.9) we get the equations for both pressure (equation of state) and density of the system with Λ -term acting as a source

$$\begin{aligned} -\Lambda g_{\mu\nu} &= 8\pi [(\rho + P)u_\mu u_\nu + P g_{\mu\nu}] \\ \implies P &= -\rho \\ \implies \rho &= \frac{\Lambda}{8\pi}. \end{aligned} \quad (2.14)$$

2.2.2 Cosmological constant Λ as an independent constant of Einstein's equations

The second option is that we look at the cosmological constant as an independent constant of the established theory. In the first case, we considered that the cosmological constant acted on the right source side as a source of curvature. The basis of this view is the idea that the established EE (1.2) contain the Newtonian gravitational constant G and the cosmological constant Λ , which characterize the gravitational interaction.

This whole Chapter is based on [Nowakowski, 2001, Weinberg, 1989, Tavora, 2020, Walters, 2016].

3. Newtonian limit

3.1 Newtonian limit without cosmological constant

We start from the geodesic equation, which can be written as [Hartle, 2002]

$$\frac{d^2 x^\nu}{d\tau^2} + \Gamma^\nu_{\mu\sigma} \frac{dx^\mu}{d\tau} \frac{dx^\sigma}{d\tau} = 0. \quad (3.1)$$

Einstein's general theory of relativity is an extension of the Newton's theory of gravity designed to cover the high speeds and areas of strong gravitational fields. In another the non-relativistic (i.e. $v \ll c$), weak gravity limit of Einstein's theory leads to Newton's theory.

The above mentioned can be characterized as

- **Weak gravitational field** - The gravitational field should be homogeneous. The weak gravitational field condition can be formulated as a slight additional perturbation $h_{\mu\nu}$ to the Minkowski space-time, described by Minkowski metric¹ Let us formulate then the covariant metric tensor as [Misner et al., 1973]

$$g_{\mu\nu} = \eta_{\mu\nu} + h_{\mu\nu}, \quad (3.3)$$

whereas the contravariant version of the metric tensor follows [Misner et al., 1973]

$$g^{\mu\nu} = \eta^{\mu\nu} - h^{\mu\nu}. \quad (3.4)$$

Let us show that both statements are consistent, i.e. that their product has to result in Kronecker delta

$$\begin{aligned} (\eta_{\mu\nu} + h_{\mu\nu})(\eta^{\nu\sigma} - h^{\nu\sigma}) &= \\ &= \delta_\mu^\sigma + h_\mu^\sigma - h_\mu^\sigma + \mathcal{O}(h^2). \end{aligned} \quad (3.5)$$

We treat $h_{\mu\nu}$ as if it were a field in Minkowski space-time and raise or lower its indices using η

$$h_\mu^\sigma = \eta^{\beta\sigma} h_{\mu\beta}. \quad (3.6)$$

We neglect the $\mathcal{O}(h^2)$ contribution to the inner product defined by eq. (3.5) as $h_{\mu\nu} \ll \eta_{\mu\nu}$. Therefore we get the same result as one would expect

¹Consider the Cartesian coordinate system in which the Minkowski metric is diagonal, that is

$$\eta_{\mu\nu} = \begin{pmatrix} -1 & 0 & 0 & 0 \\ 0 & 1 & 0 & 0 \\ 0 & 0 & 1 & 0 \\ 0 & 0 & 0 & 1 \end{pmatrix}, \quad (3.2)$$

which is described by the η_ν [Anadijiban, 1993].

when carrying out the inner product in Minkowski space-time without the perturbation.

$$\begin{aligned}
\Gamma^\nu_{\mu\sigma} &= g^{\alpha\mu}\Gamma_{\alpha\rho\sigma} \\
&= \frac{1}{2}g^{\mu\alpha}(g_{\alpha\rho,\sigma} + g_{\sigma\alpha,\rho} - g_{\rho\sigma,\alpha}) \\
&= \frac{1}{2}[\eta^{\mu\alpha} - h^{\mu\alpha}]((\eta_{\alpha\rho} + h_{\alpha\rho})_{,\sigma} + (\eta_{\sigma\alpha} + h_{\sigma\alpha})_{,\rho} - (\eta_{\rho\sigma} + h_{\rho\sigma})_{,\alpha}] \\
&= \frac{1}{2}(\eta^{\mu\alpha} - h^{\mu\alpha})(h_{\alpha\rho,\sigma} + h_{\sigma\alpha,\rho} - h_{\rho\sigma,\alpha}),
\end{aligned} \tag{3.7}$$

where we used the fact that the derivative of the Minkowski tensor is zero, so the only contributing term to the Christoffel symbols is the derivative of the term $h_{\mu\nu}$. We can delete the term $h^{\mu\alpha}$ as well because that would contribute to the result up to the term $\mathcal{O}(h^2)$. The Christoffel symbols then translate as

$$\Gamma^\nu_{\mu\sigma} = \frac{1}{2}(\eta^{\mu\alpha})(h_{\alpha\rho,\sigma} + h_{\sigma\alpha,\rho} - h_{\rho\sigma,\alpha}), \tag{3.8}$$

- **Slow movements** - This assumption dictates the spatial components of the four-velocity to be smaller than the time component of the four-velocity

$$\left|\frac{dx^i}{d\tau}\right| \ll \left|\frac{dt}{d\tau}\right|. \tag{3.9}$$

The expression given by eq. (3.9) is written in geometrized units, with the speed of the light equal to one. Contrary to the standard unit representation the term ct is substituted by t in the time component of four-velocity.

Let us write the first term in (3.9) using the coordinate time t instead of proper time τ

$$\left|\frac{dx^i}{dt}\right| \left|\frac{dt}{d\tau}\right| \ll \left|\frac{dt}{d\tau}\right| \dots |v^i| \ll c, \tag{3.10}$$

where we used the fact that Lorentz factor, defined as $\frac{dt}{d\tau}$, is non-zero and after truncation we reverse back to the standard units showing the initial velocity assumption.

We describe the geodesic equation (3.1) as

$$\frac{d^2x^\nu}{d\tau^2} + \Gamma^\nu_{00} \left(\frac{dt}{d\tau}\right)^2 + \cancel{\Gamma^\nu_{0j} \frac{dt}{d\tau} \frac{dx^j}{d\tau}} + \cancel{\Gamma^\nu_{j0} \frac{dx^j}{d\tau} \frac{dt}{d\tau}} + \cancel{\Gamma^\nu_{ji} \frac{dx^j}{d\tau} \frac{dx^i}{d\tau}} = 0. \tag{3.11}$$

where most of the terms can be neglected, because from the breakdown of the christoffel symbols given by (3.7) it is obvious that they are small because as they are of size $\mathcal{O}(h)$ and also the spatial components of four-velocity are small compared to the time component of four-velocity. It is reasonable to ignore the last three terms of the eq. (3.11), where the last term is small in all aspects discussed, i.e. in the Γ and in both four-velocity spatial components, and the second and third terms are small in the Γ and in one four-velocity spatial component. The first term is small only in the Γ and will remain present. The geodesic equation then translates as

$$\frac{d^2x^\nu}{d\tau^2} + \Gamma^\nu_{00} \left(\frac{dt}{d\tau}\right)^2 = 0. \tag{3.12}$$

Limiting ourselves to the stationary situations the metric tensor follows

$$g_{\mu\nu,0} = 0, \quad (3.13)$$

where it is obvious that the given relation is not covariant, i.e. it depends on the choice of coordinates².

Let us incorporate the latter assumption of the stationary field into non-zero components of Christoffel symbols

$$\begin{aligned} \Gamma^\nu_{00} &= \frac{1}{2} (\eta^{\mu\alpha}) (\cancel{h_{\alpha 0,0}} + \cancel{h_{0\alpha,0}} - h_{00,\alpha}) \\ &= -\frac{1}{2} h_{00}{}^{,\nu}. \end{aligned} \quad (3.14)$$

Inserting the eq. (3.14) into the eq. (3.12) we obtain Newtonian limit (hereafter NL) of the geodesic equation (3.1) as

$$\frac{d^2 x^\nu}{d\tau^2} - \frac{1}{2} h_{00}{}^{,\nu} \left(\frac{dt}{d\tau} \right)^2 = 0. \quad (3.15)$$

- **Time component** $\nu = 0$ of eq. (3.15)

$$\begin{aligned} \frac{d^2 x^0}{d\tau^2} - \frac{1}{2} h_{00}{}^{,0} \left(\frac{dt}{d\tau} \right)^2 &= 0 \\ \implies \frac{d^2 t}{d\tau^2} = 0 &\implies \frac{dt}{d\tau} = \text{const}. \end{aligned} \quad (3.16)$$

The second term from eq. (3.16) is zero due to stationary field assumption and we obtain a linear dependence between dt and $d\tau$.

- **Spatial components** $\nu = i$ of eq. (3.15)

$$\frac{d^2 x^i}{d\tau^2} - \frac{1}{2} h_{00}{}^{,i} \left(\frac{dt}{d\tau} \right)^2 = 0. \quad (3.17)$$

First of all, we solve the derivation of spatial coordinates with respect to proper time $d\tau$, so that we obtain the derivation of spatial coordinates with respect to the coordinate time dt

$$\frac{d^2 x^i}{d\tau^2} = \frac{d}{d\tau} \left(\frac{dx^i}{dt} \frac{dt}{d\tau} \right) = \frac{d^2 x^i}{dt^2} \left(\frac{dt}{d\tau} \right)^2 + \frac{dx^i}{dt} \left(\frac{d^2 t}{d\tau^2} \right). \quad (3.18)$$

The second term is equal as the eq. (3.16) holds. With this in mind we write the eq. (3.17) as

$$\frac{d^2 x^i}{dt^2} \left(\frac{dt}{d\tau} \right)^2 - \frac{1}{2} h_{00}{}^{,i} \left(\frac{dt}{d\tau} \right)^2 = 0 / \left(\frac{dt}{d\tau} \right)^2 \implies \frac{d^2 x^i}{dt^2} - \frac{1}{2} h_{00}{}^{,i} = 0, \quad (3.19)$$

where we again used the non-zero property of Lorentz factor $\frac{dt}{d\tau}$.

²The stationary field assumption is better expressed so that there are such coordinates in which the metric does not depend on time. Furthermore this coordinate system must be exactly the one in which the metric can be decomposed into a Minkowski special relativistic part and a small perturbation given by $h_{\mu\nu}$, as described in eq. (3.3).

Consider the Newtonian equation [Misner et al., 1973]

$$\frac{d^2 x^i}{dt^2} = -\phi^i. \quad (3.20)$$

If we compare this equation with NL of the geodesic equation given by (3.19) we can determine the term h_{00} , as this perturbation term is clearly related to the Newtonian potential gradient

$$h_{00} = -2\phi + \text{const}. \quad (3.21)$$

If we consider the classical Newtonian potential, it is natural to normalize it according to the needs of the given problem. We know that such a potential for an isolated system with a central body will be zero for $r \rightarrow \infty$. Alternatively if we assume that at infinity we will have a flat space-time, described by Minkowski metric, h_{00} will be zero, so the integration constant *const* has to be equal to zero as well, i.e.

$$h_{00} = -2\phi. \quad (3.22)$$

Let us insert this term into eq. (3.3) and we get

$$g_{00} = -1 - 2\phi, \quad (3.23)$$

which considering standard units translates as

$$g_{00} = -1 - \frac{2\phi}{c^2}. \quad (3.24)$$

3.2 Newtonian limit with cosmological constant

Let us formulate EE in the following form [Einstein, 1916]

$$\underbrace{R_{\mu\nu} - \frac{1}{2}Rg_{\mu\nu} + \Lambda g_{\mu\nu}}_{G_{\mu\nu}} = \kappa T_{\mu\nu}, \quad (3.25)$$

where $R_{\mu\nu}$ is the Ricci tensor, R is the Ricci scalar, $g_{\mu\nu}$ is the metric tensor, Λ is the cosmological constant and $T_{\mu\nu}$ is the energy-momentum tensor.

For our purposes it is more practical to rewrite the eq. (3.25) so that only Ricci tensor appears on the left-hand side and calculate its trace

$$\begin{aligned} g^{\mu\nu} \left(R_{\mu\nu} - \frac{1}{2}Rg_{\mu\nu} + \Lambda g_{\mu\nu} \right) &= g^{\mu\nu} (\kappa T_{\mu\nu}) \\ R - 2R + 4\Lambda &= \kappa T \\ R &= -\kappa T + 4\Lambda. \end{aligned} \quad (3.26)$$

We substitute the result of eq. (3.26) for Ricci's scalar R into the original EE (3.25), i.e.

$$\begin{aligned} R_{\mu\nu} - \frac{1}{2}(4\Lambda - \kappa T)g_{\mu\nu} + \Lambda g_{\mu\nu} &= \kappa T_{\mu\nu} \\ R_{\mu\nu} - 2\Lambda g_{\mu\nu} + \frac{1}{2}\kappa T g_{\mu\nu} + \Lambda g_{\mu\nu} &= \kappa T_{\mu\nu} \\ R_{\mu\nu} &= \kappa \left(T_{\mu\nu} - \frac{1}{2}T g_{\mu\nu} \right) + \Lambda g_{\mu\nu}. \end{aligned} \quad (3.27)$$

Next we define the Riemann tensor as [Misner et al., 1973]

$$R^\sigma_{\mu\alpha\nu} \equiv \Gamma^\sigma_{\mu\nu,\alpha} - \Gamma^\sigma_{\mu\alpha,\nu} + \Gamma^\sigma_{\beta\alpha}\Gamma^\beta_{\mu\nu} - \Gamma^\sigma_{\beta\nu}\Gamma^\beta_{\mu\alpha}. \quad (3.28)$$

Given the definition of the Riemann tensor and the definition of the Ricci tensor, which arises from the contraction of Riemann tensor in the first and the third index, we can write [Misner et al., 1973]

$$\begin{aligned} R_{\mu\nu} &\equiv R^\sigma_{\mu\sigma\nu} \\ &= \Gamma^\sigma_{\mu\nu,\sigma} - \Gamma^\sigma_{\mu\sigma,\nu} + \Gamma^\sigma_{\alpha\sigma}\Gamma^\alpha_{\mu\nu} - \Gamma^\sigma_{\alpha\nu}\Gamma^\alpha_{\mu\sigma} \\ &= \cancel{\Gamma^0_{\mu\nu,0}} + \Gamma^i_{\mu\nu,i} - \cancel{\Gamma^0_{\mu 0,\nu}} - \cancel{\Gamma^i_{\mu i,\nu}} + \cancel{\Gamma^0_{00}\Gamma^0_{\mu\nu}} + \cancel{\Gamma^0_{i0}\Gamma^i_{\mu\nu}} + \cancel{\Gamma^j_{0j}\Gamma^0_{\mu\nu}} + \\ &\quad + \cancel{\Gamma^j_{ij}\Gamma^i_{\mu\nu}} - \cancel{\Gamma^0_{0\nu}\Gamma^0_{\mu 0}} - \cancel{\Gamma^0_{i\nu}\Gamma^i_{\mu 0}} - \cancel{\Gamma^j_{0\nu}\Gamma^0_{\mu j}} - \cancel{\Gamma^j_{i\nu}\Gamma^i_{\mu j}} = \\ &= \Gamma^i_{\mu\nu,i}, \end{aligned} \quad (3.29)$$

where we used, that all Christoffel symbols are zero except Γ^i_{00} . It is thus clear from eq. (3.29) that the only choice of indices μ and ν resulting in non-zero Christoffel symbol are $\mu = 0$ and $\nu = 0$, i.e. we are left with the term $\Gamma^i_{00,i}$.

If we combine the results given by eq. (3.14) and (3.22) we can write

$$R_{00} = \Gamma^i_{00,i} = \phi^i_{,i} \equiv \Delta\phi. \quad (3.30)$$

Based on the above calculated non-zero components of the Ricci tensor we rewrite the equation (3.27) as

$$R_{00} = \kappa \left(T_{00} - \frac{1}{2} T g_{00} \right) + \Lambda g_{00}, \quad (3.31)$$

where the left-hand side is given by the eq. (3.30) and the right-hand side needs to be further expressed in the NL.

The right- hand side of eq. (3.31), therefore, contains the terms T_{00} , T and g_{00} that need to be modified. We g_{00} term is given by eq. (3.23). We formulate the remaining two terms in the NL as

- T : From the definition of the energy-momentum tensor of dust [Landau and Lifshitz, 1980] we can write

$$T^{\mu\nu}_{dust} = \rho u^\mu u^\nu. \quad (3.32)$$

We further define its trace as

$$\begin{aligned} T &= \rho u^\mu u_\mu \\ &= \rho g^{\mu\nu} u^\mu u^\nu \\ &= \rho g^{\mu\nu} \frac{dx^\mu}{d\tau} \frac{dx^\nu}{d\tau} \\ &= \rho \frac{ds^2}{d\tau^2} \\ &= -\rho, \end{aligned} \quad (3.33)$$

whereas the result is expressed in geometric units. Considering standard units we would have to multiply the density by the speed of light squared ($-\rho c^2$).

- T_{00} :

$$\begin{aligned}
T_{00} &= \rho u_0 u_0 \\
&= \rho(g_{00}u^0 + g_{0i}u^i)u_0 \\
&\doteq \rho g_{00}u^0 u_0 \\
&= \rho g_{00}(-1 - u^i u_i) \\
&\doteq -\rho g_{00} \\
&= -\rho(-1 - 2\phi) \\
&\doteq \rho,
\end{aligned} \tag{3.34}$$

where in the first approximation we considered that the time component of four-velocity is much larger than its spatial components. In the second step, we neglected the potential, which is small compared to 1. Standard unit expression would again lead to ρc^2 .

Now considering the zero cosmological constant, i.e. $\Lambda = 0$, in eq. (3.31) we get

$$\begin{aligned}
R_{00} \equiv \Delta\phi &= \kappa \left(T_{00} - \frac{1}{2} T g_{00} \right) \\
&= \kappa \left(\rho - \frac{1}{2} (-\rho)(-1 - 2\phi) \right) \\
&= \kappa \left(\rho - \frac{1}{2} \rho - \rho\phi \right) \\
&= \kappa \left(\frac{1}{2} \rho \right).
\end{aligned} \tag{3.35}$$

Poisson's equation in classical Newtonian physics in standard units is given by

$$\Delta\phi = 4\pi G\rho. \tag{3.36}$$

Comparing the eq. (3.36) and (3.35) constrains the value of constant κ to 8π , expressed in standard units as $\frac{8\pi G}{c^4}$.

Finally, let us “switch on“ the cosmological constant Λ . Considering the expressions for the Ricci tensor R_{00} and the dust energy-momentum tensor T_{00} the eq. (3.31) then translates as

$$\begin{aligned}
R_{00} \equiv \Delta\phi &= 4\pi\rho + \Lambda g_{00} \\
&= 4\pi\rho + \Lambda(-1 - 2\phi) \\
&= 4\pi\rho - \Lambda - 2\Lambda\phi \\
\Delta\phi + 2\Lambda\phi &= 4\pi\rho - \Lambda.
\end{aligned} \tag{3.37}$$

This whole Chapter is based on [Nowakowski, 2001, Weinberg, 1989, Earman, 2001].

4. Solution of the Newtonian limit

4.1 Numerical solution in Cartesian coordinates

Let's go back to Chapter 3, where we derived the NL in the form of (3.37). The second key equation is the Poisson equation

$$\Delta\phi(x, y, z) = 4\pi\rho(x, y, z), \quad (4.1)$$

Next, let's define the Laplace operator Δ in the Cartesian coordinate system as

$$\Delta = \frac{\partial^2}{\partial x^2} + \frac{\partial^2}{\partial y^2} + \frac{\partial^2}{\partial z^2}. \quad (4.2)$$

Given the definition of the Laplace operator (4.2), let's rewrite the eq. (2.10) and (4.1). For simplicity, we consider only one coordinate (e.g. x), thus replacing the full 3 dimensional solution with 1 dimensional one, still preserving the physical nature of the problem.

In the following we formulate two cases, i.e. **case I** and **case II**, where case I will correspond to a solution with Λ -term equal to zero and case II Λ -term being non-zero.

- case I

$$\frac{\partial^2\phi(x)}{\partial x^2} = 4\pi\rho(x). \quad (4.3)$$

- case II

$$\left(\frac{\partial^2}{\partial x^2} + 2\Lambda\right)\phi(x) = 4\pi\rho(x) - \Lambda. \quad (4.4)$$

Let's define Δx , where we discretize the continuous variable x

$$\Delta x = \frac{b-a}{n}; x_i = a + i\Delta x, i = 1, \dots, n-1, \quad (4.5)$$

where a and b are the initial and final value of the distance at which we will investigate the potential ϕ and n is the numerical value by which we cut the given spatial section $b-a$ into Δx_i . The larger n , the closer our solution will be to the real one, i.e. $\Delta x_i \rightarrow 0$ for $n \rightarrow \infty$.

We introduce the notation describing the physical quantities ϕ and ρ evaluated at certain point of our discretized mesh, i.e.

$$\begin{aligned} \phi_{i+1} &= \phi(x_i + \Delta x) \\ \phi_i &= \phi(x_i) \\ \phi_{i-1} &= \phi(x_i - \Delta x) \\ \rho_i &= \rho(x_i). \end{aligned} \quad (4.6)$$

Let us define the Taylor polynomial at a given point as [Weir et al., 1996]

$$\sum_{n=0}^{\infty} \frac{f^n(a)}{n!} (x - a)^n. \quad (4.7)$$

Based on the definition of (4.7), let us expand the given parts of the potential into Taylor series ($a=0$)

$$\begin{aligned} \phi_{i+1} &= \phi(x_i + \Delta x) \\ &= \phi_i + \Delta x \left. \frac{\partial \phi}{\partial x} \right|_{x=x_i} + \frac{\Delta x^2}{2!} \left. \frac{\partial^2 \phi}{\partial x^2} \right|_{x=x_i} + \frac{\Delta x^3}{3!} \left. \frac{\partial^3 \phi}{\partial x^3} \right|_{x=x_i} + \dots \end{aligned} \quad (4.8)$$

and

$$\begin{aligned} \phi_{i-1} &= \phi(x_i - \Delta x) \\ &= \phi_i - \Delta x \left. \frac{\partial \phi}{\partial x} \right|_{x=x_i} + \frac{\Delta x^2}{2!} \left. \frac{\partial^2 \phi}{\partial x^2} \right|_{x=x_i} - \frac{\Delta x^3}{3!} \left. \frac{\partial^3 \phi}{\partial x^3} \right|_{x=x_i} + \dots \end{aligned} \quad (4.9)$$

Adding the eq. (4.8) and (4.9) leads to

$$\phi_{i+1} + \phi_{i-1} = 2\phi_i + \Delta x^2 \left. \frac{\partial^2 \phi}{\partial x^2} \right|_{x=x_i} + \mathcal{O}(\Delta x^4). \quad (4.10)$$

Notice that the linear and cubic terms are subtracted from each other, so we can express from the given equations the formula for the second derivative, which appears in the Poisson equation. The term of the fourth derivative will contribute to the error of potential determination most significantly¹. For sufficiently small values of Δx (or for sufficiently large n) the error will be of the order of negligibility with respect to the constant and quadratic term [Apostol, 1967].

In the last step of this scheme we express the second derivative (4.10) as

$$\frac{\partial^2 \phi}{\partial x^2} = \frac{\phi_{i+1} - 2\phi_i + \phi_{i-1}}{\Delta x^2} + \mathcal{O}(\Delta x^2). \quad (4.11)$$

Now let us formulate the case I and II respectively

- case I

$$\begin{aligned} \frac{\partial^2 \phi(x)}{\partial x^2} &= 4\pi\rho(x) \rightarrow \\ \frac{\phi_{i+1} - 2\phi_i + \phi_{i-1}}{\Delta x^2} + \mathcal{O}(\Delta x^2) &= 4\pi\rho_i, \end{aligned} \quad (4.12)$$

where, after multiplication by the quadratic error, we obtain

$$\phi_{i+1} - 2\phi_i + \phi_{i-1} + \mathcal{O}(\Delta x^2) = \Delta x^2 4\pi\rho_i. \quad (4.13)$$

Error $\mathcal{O}(\Delta x^2)$ has been deleted based on the negligible impact on the given equation [Apostol, 1967].

¹From the nature of the definition of the Taylor polynomial, we see that only even powers contribute to the error of potential determination. All odd powers are subtracted from each other.

- case II

$$\begin{aligned} & \left(\frac{\partial^2}{\partial x^2} + 2\Lambda\right)\phi(x) = 4\pi\rho(x) - \Lambda \rightarrow \\ & \frac{\phi_{i+1} - 2\phi_i + \phi_{i-1}}{\Delta x^2} + \mathcal{O}(\Delta x^2) + 2\Lambda\phi_i = 4\pi\rho_i - \Lambda, \end{aligned} \quad (4.14)$$

where similarly to the case I (4.13), after multiplication by the quadratic error, we obtain

$$\phi_{i+1} - \phi_i(2 - 2\Lambda\Delta x^2) + \phi_{i-1} + \mathcal{O}(\Delta x^2) = \Delta x^2(4\pi\rho_i - \Lambda). \quad (4.15)$$

Based on the same discussion as in case I, we deleted the term $\mathcal{O}(\Delta x^2)$.

Eq. (4.13) and (4.14) differ from each other in one term multiplied by ϕ_i . We notice that both finite difference schemes of the Poisson equations can be unified as

$$\phi_{i+1} - \alpha\phi_i + \phi_{i-1} = \Delta x^2 4\pi\rho_i, \quad \alpha \in R. \quad (4.16)$$

Assuming Dirichlet boundary conditions the unified finite difference scheme of Poisson equation translates in matrix formalism as

$$\underbrace{\begin{pmatrix} -\alpha & 1 & 0 & 0 & 0 & \dots & \dots & 0 \\ 1 & -\alpha & 1 & 0 & 0 & \dots & \dots & 0 \\ 0 & 1 & -\alpha & 1 & 0 & \dots & \dots & 0 \\ 0 & 0 & 1 & -\alpha & 1 & \ddots & \dots & 0 \\ 0 & 0 & 0 & 1 & -\alpha & \ddots & \dots & \vdots \\ \vdots & \vdots & \vdots & \ddots & \ddots & \ddots & \ddots & \vdots \\ 0 & 0 & 0 & 0 & \ddots & \ddots & \ddots & 1 \\ 0 & 0 & 0 & 0 & 0 & 0 & 1 & -\alpha \end{pmatrix}}_{\mathbf{A}} \underbrace{\begin{pmatrix} \phi_1 \\ \phi_2 \\ \phi_3 \\ \phi_4 \\ \vdots \\ \vdots \\ \vdots \\ \phi_{n-1} \end{pmatrix}}_{\mathbf{x}} = \underbrace{\begin{pmatrix} \Delta x^2(4\pi\rho_1 - \Lambda) - \phi_0 \\ \Delta x^2(4\pi\rho_2 - \Lambda) \\ \Delta x^2(4\pi\rho_3 - \Lambda) \\ \Delta x^2(4\pi\rho_4 - \Lambda) \\ \vdots \\ \vdots \\ \vdots \\ \Delta x^2(4\pi\rho_{n-1} - \Lambda) - \phi_n \end{pmatrix}}_{\mathbf{b}}. \quad (4.17)$$

We obtained the matrix equation $\mathbf{A}\vec{x} = \vec{b}$. Now solving the system of linear equations given by (4.17) will present us with the potential ϕ .

The solution for the required potential ϕ is conditioned by choosing both the initial and final value of potential ϕ_0 and ϕ_n , respectively, as well as the density profile ρ . We are interested in the change of the potential behaviour based on solutions when $\Lambda = 0$ and $\Lambda \neq 0$, i.e. the case of a modified Poisson equation with a Λ -term.

4.2 Numerical solution in Spherical coordinates

In a similar way as in sub-section 4.1, we derive a solution in Spherical coordinates. We will start from the Poisson equation in the form (4.1) and the NL (3.37). The Laplace operator in Spherical coordinates reads as

$$\Delta = \frac{1}{r^2} \frac{\partial}{\partial r} \left(r^2 \frac{\partial}{\partial r} \right) + \frac{1}{r^2 \sin(\theta)} \frac{\partial}{\partial \theta} \left(\sin(\theta) \frac{\partial}{\partial \theta} \right) + \frac{1}{r^2 \sin^2(\theta)} \frac{\partial^2}{\partial \varphi^2}, \quad (4.18)$$

Eq. (4.18) depends on three variables r , θ and φ . For simplicity, considering the spherical symmetry, i.e. $\frac{\partial}{\partial\theta} = \frac{\partial}{\partial\varphi} = 0$, we write

$$\Delta = \frac{1}{r^2} \frac{\partial}{\partial r} \left(r^2 \frac{\partial\phi(r)}{\partial r} \right) = \frac{\partial^2\phi(r)}{\partial r^2} + \frac{2}{r} \frac{\partial\phi(r)}{\partial r}. \quad (4.19)$$

Applying the spherical Laplace given by (4.19) to case I and case II we obtain

- case I

$$\Delta\phi(r) = r \frac{\partial^2\phi(r)}{\partial r^2} + 2 \frac{\partial\phi(r)}{\partial r} = 4\pi\rho(r)r. \quad (4.20)$$

- case II

$$\begin{aligned} (\Delta + 2\Lambda)\phi(r) &= r \frac{\partial^2\phi(r)}{\partial r^2} + 2 \frac{\partial\phi(r)}{\partial r} + 2\Lambda r\phi(r) \\ &= (4\pi\rho(r) - \Lambda)r. \end{aligned} \quad (4.21)$$

Similar to Cartesian coordinates, let's discretize Δr

$$\Delta r = \frac{b-a}{n}; r_i = a + i\Delta r, i = 1, \dots, n-1. \quad (4.22)$$

Taking similar steps for the evaluation of potential ϕ and density ρ at the certain points of our discretized mesh we define

$$\begin{aligned} \phi_{i+1} &= \phi(r_i + \Delta r) \\ \phi_i &= \phi(r_i) \\ \phi_{i-1} &= \phi(r_i - \Delta r) \\ \rho_i &= \rho(r_i). \end{aligned} \quad (4.23)$$

Let's expand the potentials ϕ_{i+1} and ϕ_{i-1} into the Taylor series as

$$\begin{aligned} \phi_{i+1} &= \phi(r_i + \Delta r) \\ &= \phi_i + \Delta r \frac{\partial\phi}{\partial r} \Big|_{r=r_i} + \frac{\Delta r^2}{2!} \frac{\partial^2\phi}{\partial r^2} \Big|_{r=r_i} + \frac{\Delta r^3}{3!} \frac{\partial^3\phi}{\partial r^3} \Big|_{r=r_i} + \dots \end{aligned} \quad (4.24)$$

and

$$\begin{aligned} \phi_{i-1} &= \phi(r_i - \Delta r) \\ &= \phi_i - \Delta r \frac{\partial\phi}{\partial r} \Big|_{r=r_i} + \frac{\Delta r^2}{2!} \frac{\partial^2\phi}{\partial r^2} \Big|_{r=r_i} - \frac{\Delta r^3}{3!} \frac{\partial^3\phi}{\partial r^3} \Big|_{r=r_i} + \dots \end{aligned} \quad (4.25)$$

In order to express the second and first derivatives in spherically symmetric variations of the Poisson equation, it is necessary to define the difference and the sum of the eq. (4.24) and (4.25)

$$\phi_{i+1} + \phi_{i-1} = 2\phi_i + \Delta r^2 \frac{\partial^2\phi}{\partial r^2} \Big|_{r=r_i} + \mathcal{O}(\Delta r^4) \quad (4.26)$$

and

$$\phi_{i+1} - \phi_{i-1} = 2\Delta r \frac{\partial\phi}{\partial r} \Big|_{r=r_i} + \mathcal{O}(\Delta r^3). \quad (4.27)$$

The expression (4.26) involves the error $\mathcal{O}(\Delta r^4)$ in the same way as it was with Cartesian coordinates. Additional term that will contribute to the error of determining the second derivative in the Poisson equations will be $\mathcal{O}(\Delta r^6)$. In another words, all even powers. A similar discussion based on [Weir et al., 1996] will rule out these errors compared to the largest term. The expression (4.27) is already burdened by a third-order error, as these powers add up to (4.26). Thus, the determination of the first derivative, which is moreover found in the spherical expression of the Poisson equation, as opposed to the Cartesian expression, is burdened by all odd powers from the third order. Due to the nature of the problem, we will neglect all these powers compared to the largest term [Weir et al., 1996].

We re-formulate case I and case II

- case I

$$\begin{aligned}
& r \frac{\partial^2 \phi(r)}{\partial r^2} + 2 \frac{\partial \phi(r)}{\partial r} = 4\pi \rho(r) r \rightarrow \\
& r_i \frac{\phi_{i+1} - 2\phi_i + \phi_{i-1}}{\Delta r^2} + \frac{\phi_{i+1} - \phi_{i-1}}{\Delta r} + \mathcal{O}(\Delta r^2) = 4\pi \rho_i r_i \\
& \phi_{i+1} \left(\frac{r_i}{\Delta r^2} + \frac{1}{\Delta r} \right) - \phi_i \frac{2r_i}{\Delta r^2} + \phi_{i-1} \left(\frac{r_i}{\Delta r^2} - \frac{1}{\Delta r} \right) + \mathcal{O}(\Delta r^2) = 4\pi \rho_i r_i,
\end{aligned} \tag{4.28}$$

where the error $\mathcal{O}(\Delta r^2)$ was neglected [Weir et al., 1996]. For simplicity we define four variables, which multiply the individual parts of the potentials evaluated at certain mesh points, i.e.

$$\begin{aligned}
\alpha_i^I &= \frac{r_i}{\Delta r^2} + \frac{1}{\Delta r} \\
\beta_i^I &= \frac{2r_i}{\Delta r^2} \\
\gamma_i^I &= \frac{r_i}{\Delta r^2} - \frac{1}{\Delta r} \\
\delta_i^I &= 4\pi \rho_i r_i.
\end{aligned} \tag{4.29}$$

Now let's rewrite eq. (4.28) using α_i^I , β_i^I , γ_i^I and δ_i^I as in eq. (4.29).

$$\alpha_i^I \phi_{i+1} - \beta_i^I \phi_i + \gamma_i^I \phi_{i-1} + \mathcal{O}(\Delta r^2) = \delta_i^I. \tag{4.30}$$

- case II

$$\begin{aligned}
& \left(r \frac{\partial^2}{\partial r^2} + 2 \frac{\partial}{\partial r} + 2\Lambda r \right) \phi(r) = (4\pi \rho(r) - \Lambda) r \rightarrow \\
& r_i \frac{\phi_{i+1} - 2\phi_i + \phi_{i-1}}{\Delta r^2} + \frac{\phi_{i+1} - \phi_{i-1}}{\Delta r} + \mathcal{O}(\Delta r^2) + 2\Lambda r_i \phi_i = \\
& \hspace{15em} (4\pi \rho_i - \Lambda) r_i \\
& \phi_{i+1} \left(\frac{r_i}{\Delta r^2} + \frac{1}{\Delta r} \right) - \phi_i \left(\frac{2r_i}{\Delta r^2} - 2\Lambda r_i \right) + \phi_{i-1} \left(\frac{r_i}{\Delta r^2} - \frac{1}{\Delta r} \right) + \mathcal{O}(\Delta r^2) = \\
& \hspace{15em} (4\pi \rho_i - \Lambda) r_i.
\end{aligned} \tag{4.31}$$

Similarly define the variables that multiply the individual parts of the potentials evaluated at certain mesh points in eq. (4.31)

$$\begin{aligned}
\alpha_i^{\text{II}} &= \frac{r_i}{\Delta r^2} + \frac{1}{\Delta r} \\
\beta_i^{\text{II}} &= \frac{2r_i}{\Delta r^2} - 2\Lambda r_i \\
\gamma_i^{\text{II}} &= \frac{r_i}{\Delta r^2} - \frac{1}{\Delta r} \\
\delta_i^{\text{II}} &= (4\pi\rho_i - \Lambda)r_i.
\end{aligned} \tag{4.32}$$

Further we write eq. (4.31) using α_i^{II} , β_i^{II} , γ_i^{II} and δ_i^{II} from eq. (4.32)

$$\alpha_i^{\text{II}}\phi_{i+1} - \beta_i^{\text{II}}\phi_i + \gamma_i^{\text{II}}\phi_{i-1} = \delta_i^{\text{II}}. \tag{4.33}$$

Comparing the case I and case II leads unification of finite difference scheme as follows

$$\begin{aligned}
\alpha_i^{\text{I}} &= \alpha_i^{\text{II}} \equiv \alpha_i \\
\beta_i^{\text{I}} &\neq \beta_i^{\text{II}} \\
\gamma_i^{\text{I}} &= \gamma_i^{\text{II}} \equiv \gamma_i \\
\delta_i^{\text{I}} &\neq \delta_i^{\text{II}}
\end{aligned} \tag{4.34}$$

$$\alpha_i\phi_{i+1} - \beta_i^{\text{I/II}}\phi_i + \gamma_i\phi_{i-1} = \delta_i^{\text{I/II}}. \tag{4.35}$$

Assuming Dirichlet boundary conditions the unified finite difference scheme of Poisson equation translates in matrix formalism as

$$\begin{pmatrix}
-\beta_1^{\text{I/II}} & \alpha_1 & 0 & 0 & 0 & \dots & \dots & 0 \\
\gamma_2 & -\beta_2^{\text{I/II}} & \alpha_2 & 0 & 0 & \dots & \dots & 0 \\
0 & \gamma_3 & -\beta_3^{\text{I/II}} & \alpha_3 & 0 & \dots & \dots & 0 \\
0 & 0 & \gamma_4 & -\beta_4^{\text{I/II}} & \alpha_4 & \ddots & \dots & 0 \\
0 & 0 & 0 & \gamma_5 & -\beta_5^{\text{I/II}} & \ddots & \dots & \vdots \\
\vdots & \vdots & \vdots & \ddots & \ddots & \ddots & \ddots & \vdots \\
0 & 0 & 0 & 0 & \ddots & \ddots & \ddots & \alpha_{n-2} \\
0 & 0 & 0 & 0 & 0 & 0 & \gamma_{n-1} & -\beta_{n-1}^{\text{I/II}}
\end{pmatrix} \cdot \begin{pmatrix} \phi_1 \\ \phi_2 \\ \phi_3 \\ \phi_4 \\ \vdots \\ \vdots \\ \vdots \\ \phi_{n-2} \\ \phi_{n-1} \end{pmatrix} = \begin{pmatrix} \delta_1^{\text{I/II}} - \gamma_1\phi_0 \\ \delta_2^{\text{I/II}}r_2 \\ \delta_3^{\text{I/II}}r_3 \\ \delta_4^{\text{I/II}}r_4 \\ \vdots \\ \vdots \\ \vdots \\ \delta_{n-2}^{\text{I/II}} \\ \delta_{n-1}^{\text{I/II}} - \alpha_{n-1}\phi_n \end{pmatrix}. \tag{4.36}$$

Now solving the system of linear equations given by (4.36) will present us with the potential ϕ represented in Spherical coordinates.

4.3 Numerical solution in Polar coordinates

The last case of coordinates system in which we will investigate the Poisson equations are Polar coordinates. Let's define the Laplace operator in Polar coordinates as follows

$$\Delta(f) = \frac{1}{r} \frac{\partial}{\partial r} \left(r \frac{\partial}{\partial r} \right) (f) + \frac{1}{r^2} \frac{\partial}{\partial \theta} \left(\frac{\partial}{\partial \theta} \right) (f). \quad (4.37)$$

The expression (4.37) depends on two variables r and θ . Assuming axial symmetry, i.e. $\frac{\partial}{\partial \theta} = 0$, the Laplace operator translates as

$$\Delta = \frac{1}{r} \frac{\partial}{\partial r} \left(r \frac{\partial}{\partial r} \right) = \frac{\partial^2 \phi(r)}{\partial r^2} + \frac{1}{r} \frac{\partial \phi(r)}{\partial r}. \quad (4.38)$$

Applying the polar Laplace given by (4.38) to case I and case II we obtain

- case I

$$\Delta \phi(r) = r \frac{\partial^2 \phi(r)}{\partial r^2} + \frac{\partial \phi(r)}{\partial r} = 4\pi \rho(r)r. \quad (4.39)$$

- case II

$$\begin{aligned} (\Delta + 2\Lambda)\phi(r) &= r \frac{\partial^2 \phi(r)}{\partial r^2} + \frac{\partial \phi(r)}{\partial r} + 2\Lambda r \phi(r) \\ &= (4\pi \rho(r) - \Lambda)r. \end{aligned} \quad (4.40)$$

In a similar way, we introduce a discrete variable Δr^2 , such as

$$\Delta r = \frac{b-a}{n}; r_i = a + i\Delta r, i = 1, \dots, n-1. \quad (4.41)$$

We introduce the notation describing the physical quantities ϕ and ρ evaluated at certain point of our discretized mesh, i.e.

$$\begin{aligned} \phi_{i+1} &= \phi(r_i + \Delta r) \\ \phi_i &= \phi(r_i) \\ \phi_{i-1} &= \phi(r_i - \Delta r) \\ \rho_i &= \rho(r_i). \end{aligned} \quad (4.42)$$

We expand the potentials ϕ_{i+1} and ϕ_{i-1} in the Taylor series

$$\begin{aligned} \phi_{i+1} &= \phi(r_i + \Delta r) \\ &= \phi_i + \Delta r \frac{\partial \phi}{\partial r} \Big|_{r=r_i} + \frac{\Delta r^2}{2!} \frac{\partial^2 \phi}{\partial r^2} \Big|_{r=r_i} + \frac{\Delta r^3}{3!} \frac{\partial^3 \phi}{\partial r^3} \Big|_{r=r_i} + \dots \end{aligned} \quad (4.43)$$

and

$$\begin{aligned} \phi_{i-1} &= \phi(r_i - \Delta r) \\ &= \phi_i - \Delta r \frac{\partial \phi}{\partial r} \Big|_{r=r_i} + \frac{\Delta r^2}{2!} \frac{\partial^2 \phi}{\partial r^2} \Big|_{r=r_i} - \frac{\Delta r^3}{3!} \frac{\partial^3 \phi}{\partial r^3} \Big|_{r=r_i} + \dots \end{aligned} \quad (4.44)$$

²The notation is the same as for Spherical coordinates, because it is essentially the same variable.

Laplace in Polar coordinates (4.38) contains similarly as Laplace in Spherical coordinates the first and second derivative, therefore it is necessary to subtract the eq. (4.43) and (4.44) and add them once again to obtain the respective derivatives.

$$\phi_{i+1} + \phi_{i-1} = 2\phi_i + \Delta r^2 \frac{\partial^2 \phi}{\partial r^2} \Big|_{r=r_i} + \mathcal{O}(\Delta r^4) \quad (4.45)$$

and

$$\phi_{i+1} - \phi_{i-1} = 2\Delta r \frac{\partial \phi}{\partial r} \Big|_{r=r_i} + \mathcal{O}(\Delta r^3). \quad (4.46)$$

The expression (4.45) involves even powers of errors from the fourth upwards, while due to the same discussion as in the case of Spherical coordinates higher powers are neglected against the largest term. The same discussion applies to the eq. (4.46), which is burdened with odd errors from the third order upwards.

Given the above, let's define case I and case II for Polar coordinates

- case I

$$\begin{aligned} r \frac{\partial^2 \phi(r)}{\partial r^2} + \frac{\partial \phi(r)}{\partial r} &= 4\pi \rho(r)r \rightarrow \\ r_i \frac{\phi_{i+1} - 2\phi_i + \phi_{i-1}}{\Delta r^2} + \frac{\phi_{i+1} - \phi_{i-1}}{2\Delta r} + \mathcal{O}(\Delta r^2) &= 4\pi \rho_i r_i \\ \phi_{i+1} \left(\frac{r_i}{\Delta r^2} + \frac{1}{2\Delta r} \right) - \phi_i \frac{2r_i}{\Delta r^2} + \phi_{i-1} \left(\frac{r_i}{\Delta r^2} - \frac{1}{2\Delta r} \right) + \mathcal{O}(\Delta r^2) &= 4\pi \rho_i r_i. \end{aligned} \quad (4.47)$$

In eq. (4.47) we define the variables that multiply the individual parts of the potentials evaluated at certain mesh points as

$$\begin{aligned} \alpha_i^I &= \frac{r_i}{\Delta r^2} + \frac{1}{2\Delta r} \\ \beta_i^I &= \frac{2r_i}{\Delta r^2} \\ \gamma_i^I &= \frac{r_i}{\Delta r^2} - \frac{1}{2\Delta r} \\ \delta_i^I &= 4\pi \rho_i r_i. \end{aligned} \quad (4.48)$$

Let's rewrite the eq. (4.47) using the introduced variables $\alpha_i^I, \beta_i^I, \gamma_i^I$ and δ_i^I as

$$\alpha_i^I \phi_{i+1} - \beta_i^I \phi_i + \gamma_i^I \phi_{i-1} = \delta_i^I. \quad (4.49)$$

- case II

$$\begin{aligned} \left(r \frac{\partial^2}{\partial r^2} + \frac{\partial}{\partial r} + 2\Lambda r \right) \phi(r) &= (4\pi \rho(r) - \Lambda)r \rightarrow \\ r_i \frac{\phi_{i+1} - 2\phi_i + \phi_{i-1}}{\Delta r^2} + \frac{\phi_{i+1} - \phi_{i-1}}{2\Delta r} + \mathcal{O}(\Delta r^2) + 2\Lambda r_i \phi_i &= \\ &= (4\pi \rho_i - \Lambda)r_i \\ \phi_{i+1} \left(\frac{r_i}{\Delta r^2} + \frac{1}{2\Delta r} \right) - \phi_i \left(\frac{2r_i}{\Delta r^2} - 2\Lambda r_i \right) + \phi_{i-1} \left(\frac{r_i}{\Delta r^2} - \frac{1}{2\Delta r} \right) + \mathcal{O}(\Delta r^2) &= \\ &= (4\pi \rho_i - \Lambda)r_i. \end{aligned} \quad (4.50)$$

Let's define the following

$$\begin{aligned}
\alpha_i^{\text{II}} &= \frac{r_i}{\Delta r^2} + \frac{1}{2\Delta r} \\
\beta_i^{\text{II}} &= \frac{2r_i}{\Delta r^2} - 2\Lambda r_i \\
\gamma_i^{\text{II}} &= \frac{r_i}{\Delta r^2} - \frac{1}{2\Delta r} \\
\delta_i^{\text{II}} &= (4\pi\rho_i - \Lambda)r_i.
\end{aligned} \tag{4.51}$$

Given the definition of the variables by eq. (4.51), let's rewrite the eq. (4.50) as

$$\alpha_i^{\text{II}}\phi_{i+1} - \beta_i^{\text{II}}\phi_i + \gamma_i^{\text{II}}\phi_{i-1} = \delta_i^{\text{II}}. \tag{4.52}$$

As in the case of the spherical equivalent of the Poisson equation we compare the defined variables for case I and case II, i.e.

$$\begin{aligned}
\alpha_i^{\text{I}} &= \alpha_i^{\text{II}} = \alpha_i \\
\beta_i^{\text{I}} &\neq \beta_i^{\text{II}} \\
\gamma_i^{\text{I}} &= \gamma_i^{\text{II}} = \gamma_i \\
\delta_i^{\text{I}} &\neq \delta_i^{\text{II}}.
\end{aligned} \tag{4.53}$$

We further define unified finite difference scheme as

$$\alpha_i\phi_{i+1} - \beta_i^{\text{I/II}}\phi_i + \gamma_i\phi_{i-1} = \delta_i^{\text{I/II}}. \tag{4.54}$$

Assuming Dirichlet boundary conditions the unified finite difference scheme of Poisson equation translates in matrix formalism as

$$\begin{pmatrix}
-\beta_1^{\text{I/II}} & \alpha_1 & 0 & 0 & 0 & \dots & \dots & 0 \\
\gamma_2 & -\beta_2^{\text{I/II}} & \alpha_2 & 0 & 0 & \dots & \dots & 0 \\
0 & \gamma_3 & -\beta_3^{\text{I/II}} & \alpha_3 & 0 & \dots & \dots & 0 \\
0 & 0 & \gamma_4 & -\beta_4^{\text{I/II}} & \alpha_4 & \ddots & \dots & 0 \\
0 & 0 & 0 & \gamma_5 & -\beta_5^{\text{I/II}} & \ddots & \dots & \vdots \\
\vdots & \vdots & \vdots & \ddots & \ddots & \ddots & \ddots & \vdots \\
0 & 0 & 0 & 0 & \ddots & \ddots & \ddots & \alpha_{n-2} \\
0 & 0 & 0 & 0 & 0 & 0 & \gamma_{n-1} & -\beta_{n-1}^{\text{I/II}}
\end{pmatrix} \cdot \begin{pmatrix} \phi_1 \\ \phi_2 \\ \phi_3 \\ \phi_4 \\ \vdots \\ \vdots \\ \vdots \\ \phi_{n-2} \\ \phi_{n-1} \end{pmatrix} = \begin{pmatrix} \delta_1^{\text{I/II}} - \gamma_1\phi_0 \\ \delta_2^{\text{I/II}} \\ \delta_3^{\text{I/II}} \\ \delta_4^{\text{I/II}} \\ \vdots \\ \vdots \\ \vdots \\ \delta_{n-2}^{\text{I/II}} \\ \delta_{n-1}^{\text{I/II}} - \alpha_{n-1}\phi_n \end{pmatrix}. \tag{4.55}$$

Now solving the system of linear equations given by (4.55) will present us with the potential ϕ represented in Polar coordinates.

5. Results

We show the behaviour of the numerically solved potential for both cases – with and without the cosmological constant Λ . We also discuss the differences between the two potentials for the case of Spherical and Polar coordinates.

In order to be able to compare the individual numerical solutions we need to know at least one analytical solution to the problems. We will take the solution of eq. (3.37) and (2.1) for the vacuum, for the case of spherical symmetry, as the starting analytical solution. Thus, we require an accurate vacuum analytical solution for NL

$$\frac{1}{r^2} \frac{d}{dr} \left(r^2 \frac{d}{dr} \right) \phi + 2\Lambda\phi = -\Lambda \quad (5.1)$$

and accurate vacuum analytical solution for Poisson equation

$$\frac{1}{r^2} \frac{d}{dr} \left(r^2 \frac{d}{dr} \right) \phi = 0. \quad (5.2)$$

The analytical solution of eq. (5.1) can be derived due to the knowledge of the analytical solution for the so-called Yukawa potential. This potential was derived by Hideki Yukawa in 1934 for case of the potential that describes the field of nuclear forces [Yukawa, 1935]. The analytical solution for the spherically symmetric case (5.1) is given by (see in detail Appendix A.1)

$$\phi_{vacuum}(r) = \frac{\bar{A}}{r} \cos\sqrt{2\Lambda}r + \frac{\bar{C}}{r} \sin\sqrt{2\Lambda}r - \frac{1}{2}. \quad (5.3)$$

The difference between solutions (5.3) and the solution for the classical Newtonian potential for vacuum case (see in detail Appendix A.2) follows

$$\sim (\sqrt{2\Lambda}r) - \frac{(\sqrt{2\Lambda}r)^2}{2!} - \frac{(\sqrt{2\Lambda}r)^3}{3!}. \quad (5.4)$$

If we take into account the current size of Λ ($\Lambda \approx 10^{-56} \text{ cm}^{-2}$ [Kohn, 2020]), the ratio of the leading term $(\sqrt{2\Lambda}r)^1$, which contributes to the difference of both solved potentials the most, is for small distances the following

- **Sun-Jupiter distance:** On scales up to the distance of Jupiter from the sun ($\sim 7 \times 10^{13} \text{ cm}$ [Nasa, 2021a]), for vacuum case, we can assume

$$\begin{aligned} \frac{\frac{(\sqrt{2\Lambda}r)^2}{2!} + \frac{(\sqrt{2\Lambda}r)^3}{3!}}{(\sqrt{2\Lambda}r)} &\approx \Lambda^{\frac{1}{2}}r + \Lambda r^2 \approx 10^{-28} \times 10^{13} + 10^{-56} \times 10^{26} \\ &\approx 10^{-15} + 10^{-30} \approx 10^{-15}. \end{aligned} \quad (5.5)$$

We see that the worst case scenario on Sun-Jupiter scales will cause a maximum error of 10^{-15} .

¹If we define small spatial scales up to the size of our galaxy, which is about $\sim 10^{23} \text{ cm}$, then the term $(\sqrt{2\Lambda}r)$ is indeed the dominant term (i.e. in the worst case scenario) and still an order of magnitude 10^{-5} larger than the next term $\frac{(\sqrt{2\Lambda}r)^2}{2!}$.

- **Sun-Voyager I distance:** On scales up to the distance of Voyager I from the sun ($\sim 2 \times 10^{15}$ cm [Nasa, 2021b]), for vacuum case, we can assume

$$\frac{\frac{(\sqrt{2\Lambda}r)^2}{2!} + \frac{(\sqrt{2\Lambda}r)^3}{3!}}{(\sqrt{2\Lambda}r)} \approx \Lambda^{\frac{1}{2}}r + \Lambda r^2 \approx 10^{-28} \times 10^{15} + 10^{-56} \times 10^{30} \quad (5.6)$$

$$\approx 10^{-13} + 10^{-26} \approx 10^{-13}.$$

We see that the worst case scenario on Sun-Voyager I scales will cause a maximum error of 10^{-13} .

- **Distance of the gravitational interaction of the sun:** Considering the characteristic scales between ~ 0 cm and $\sim 2 \times 10^{18}$ cm [Nasa, 2021c], which is approximately the upper limit of the gravitational interaction of the sun

$$\frac{\frac{(\sqrt{2\Lambda}r)^2}{2!} + \frac{(\sqrt{2\Lambda}r)^3}{3!}}{(\sqrt{2\Lambda}r)} \approx \Lambda^{\frac{1}{2}}r + \Lambda r^2 \approx 10^{-28} \times 10^{18} + 10^{-56} \times 10^{36} \quad (5.7)$$

$$\approx 10^{-10} + 10^{-20} \approx 10^{-10}.$$

We see that the worst case scenario, the scale of the order of the outer edge of the solar system will cause, corresponds to a maximum error of 10^{-10} .

- **The dimensions of our galaxy:** The characteristic dimensions of galaxies in space are variable. However, we consider distances proportional to the radius of our galaxy, which are $\sim 10^{23}$ cm [Coffey, 2010]

$$\frac{\frac{(\sqrt{2\Lambda}r)^2}{2!} + \frac{(\sqrt{2\Lambda}r)^3}{3!}}{(\sqrt{2\Lambda}r)} \approx \Lambda^{\frac{1}{2}}r + \Lambda r^2 \approx 10^{-28} \times 10^{23} + 10^{-56} \times 10^{46} \quad (5.8)$$

$$\approx 10^{-5} + 10^{-10} \approx 10^{-5}.$$

The worst case scenario that can occur at such a distance is proportional to the error 10^{-5} .

We calculated two potentials – without Λ , denoted as $\phi_{\text{unperturbed}}$ and the potential with Λ denoted as $\phi_{\text{perturbed}}$. In total, we considered four distance scales, namely the Sun-Jupiter distance, the Sun-Voyager I distance, the radius of solar system and the radius of our galaxy. Each case was analyzed for the following density profiles to $\rho = 0$, $\rho = \text{const}$, $\rho \propto r$ and $\rho \propto \frac{1}{r}$.

5.1 Sun-Jupiter distance

For the Sun-Jupiter distance, we observe large deviation between $\phi_{\text{unperturbed}}$ and $\phi_{\text{perturbed}}$ in the case of zero density. For long distances, both potentials are close to zero, which are reasonable boundary conditions. Given the analytical solutions (5.1) and (5.2), we are able to determine the expected difference between the two potentials in the case of vacuum assuming spherical symmetry. The difference will be given by the leading term ($\sqrt{2\Lambda}r$), which for the distance 5.2 Au is at the level of 10^{-14} . The numerical method described in Chapter 4 gives identical results for the selected case (see Figure 5.1).

After adding the mass to the problem, the difference between the calculated potentials is reduced by several orders of magnitude. However, this is not the case in general. In the case of constant density the potential difference shifts to the level of 10^{-16} (see Figure 5.2). For a linearly decreasing density, the difference is at the 10^{-15} level (see Figure 5.4). However, if we consider a linearly increasing density with distance, then the difference increases by one order of power ($\sim 10^{-13}$). This phenomenon is probably due to the above-discussed character of Λ , which acts against gravity, i.e. against matter (see Figure 5.3).

We do not observe a significant change in results given different choice of coordinates. However, changing the coordinate system causes a shift in the distance where the maximum difference between the calculated potentials takes place.

However, the plotted differences $\phi_{\text{unperturbed}}$ and $\phi_{\text{perturbed}}$ are at the limit of measurability with respect to the double precision, i.e. at the level of 10^{-16} . The differences vary with respect to the given density profile. At such small distances, the density profile is highly unbalanced, which is likely to shift the difference towards the limit value 10^{-16} compared to the vacuum solution. Despite the different density profiles, we should not reach smaller differences than 10^{-16} , and therefore even at such a short distance it should be possible to detect the cosmological constant Λ .

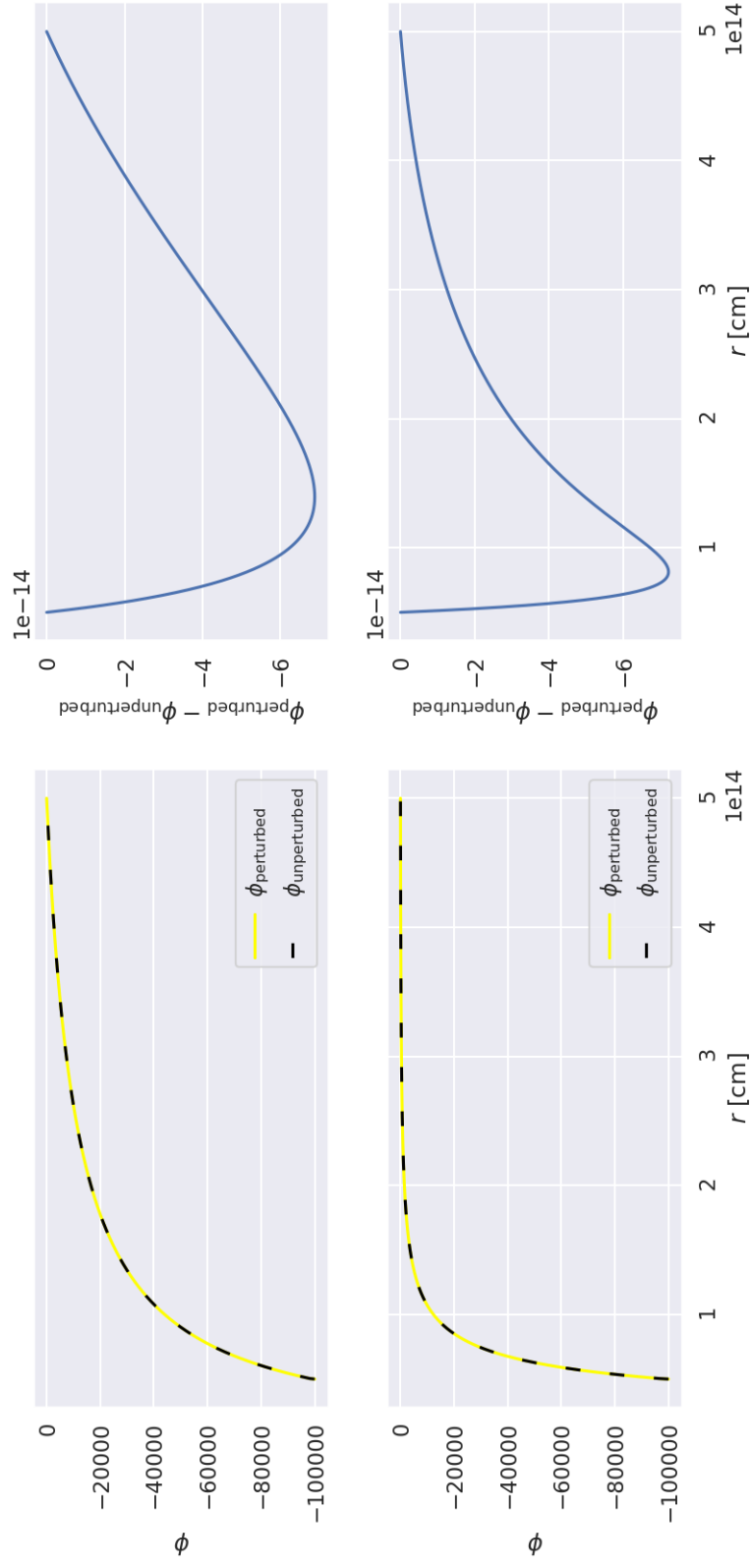


Figure 5.1: Numerical solution (distance Sun to Jupiter $\propto 5$ AU) – Spherical coordinates (top panel), Polar coordinates (bottom panel). Both calculations are carried out with the density profile $\rho = 0$.

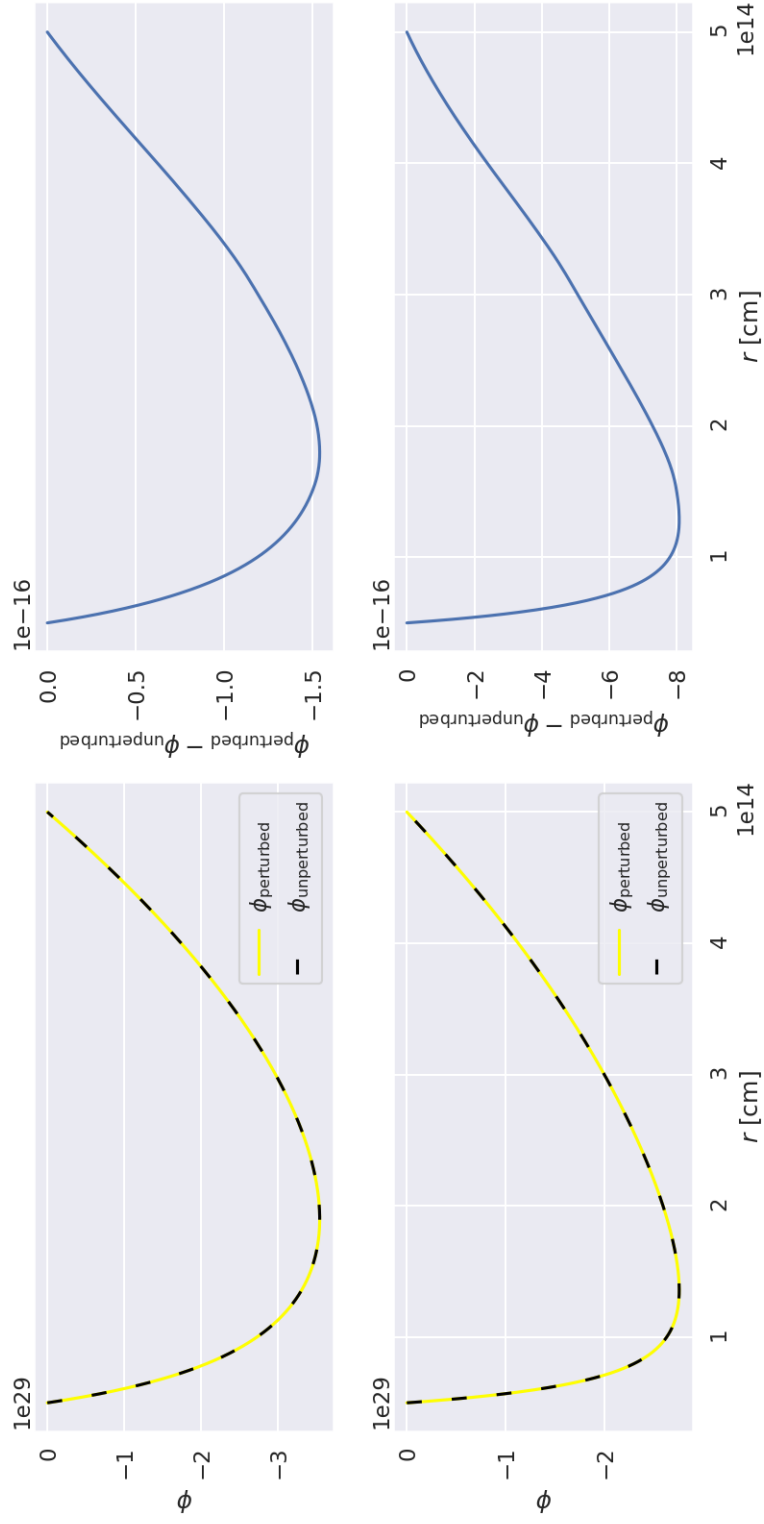


Figure 5.2: Numerical solution (distance Sun to Jupiter $\propto 5 \text{ AU}$) – Spherical coordinates (top panel), Polar coordinates (bottom panel). Both calculations are carried out with the density profile $\rho \propto \text{const}$ ($\text{const} = 1$).

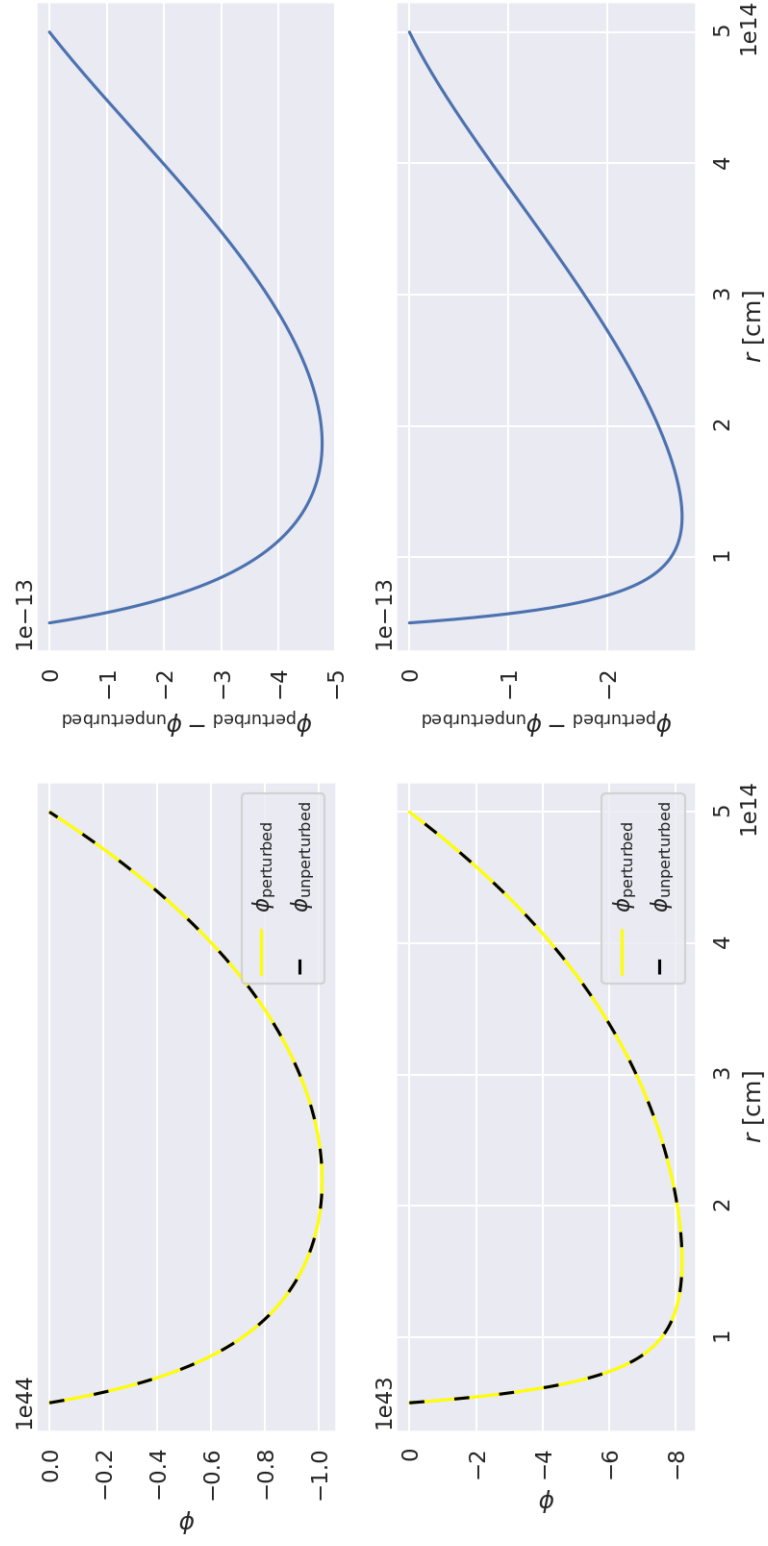


Figure 5.3: Numerical solution (distance Sun to Jupiter $\propto 5$ AU) – Spherical coordinates (top panel), Polar coordinates (bottom panel). Both calculations are carried out with the density profile $\rho \propto r$.

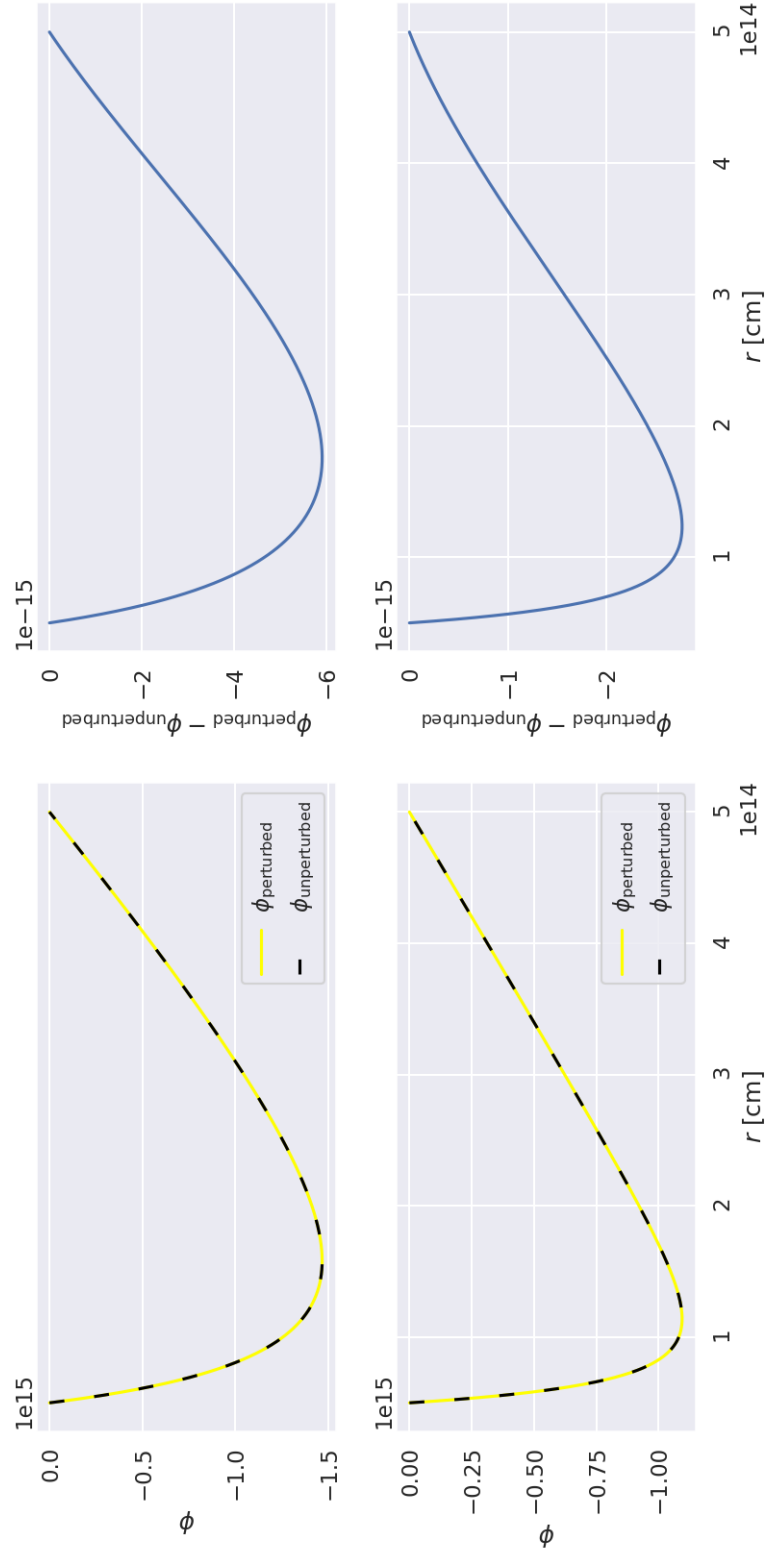


Figure 5.4: Numerical solution (distance Sun to Jupiter $\propto 5$ AU) – Spherical coordinates (top panel), Polar coordinates (bottom panel). Both calculations are carried out with the density profile $\rho \propto \frac{1}{r}$.

5.2 Sun-Voyager I distance

In the case of the Sun-Voyager I distance we observe large deviation between $\phi_{\text{unperturbed}}$ and $\phi_{\text{perturbed}}$ in the case of zero density. For long distances, both potentials are close to zero, which are reasonable boundary conditions. Given the analytical solutions (5.1) and (5.2), we are able to determine the expected difference between the two potentials in the case of vacuum assuming spherical symmetry. The difference will be given by the leading term ($\sqrt{2\Lambda}r$) (same as for Sun-Jupiter distance), which for the distance 150 Au is at the level of 10^{-13} . The numerical method described in Chapter 4 gives identical results for the selected case (see Figure 5.5).

The difference between the numerically calculated potentials begins to change with respect to the density profile. In the case of constant density the potential difference shifts to the level of 10^{-15} (see Figure 5.6). For linearly decreasing density, the difference is at 10^{-14} (see Figure 5.8). However, if we consider linearly increasing density profile the difference increases almost by one order, which is exactly same result as in the case of Sun-Jupiter distance. This phenomenon is probably due to the above-discussed character of Λ acting against gravity, i.e. against matter (see Figure 5.7).

Different density profiles influence the differences of potentials $\phi_{\text{unperturbed}}$ and $\phi_{\text{perturbed}}$ in detectable values, i.e. above the double precision level. However, it is necessary to consider more realistic profiles to describe the density distribution between the sun and Voyager I.

We do not observe a significant change in results given different choice of coordinates. Changing the coordinate system causes a shift in the distance where the maximum difference between the calculated potentials takes place.

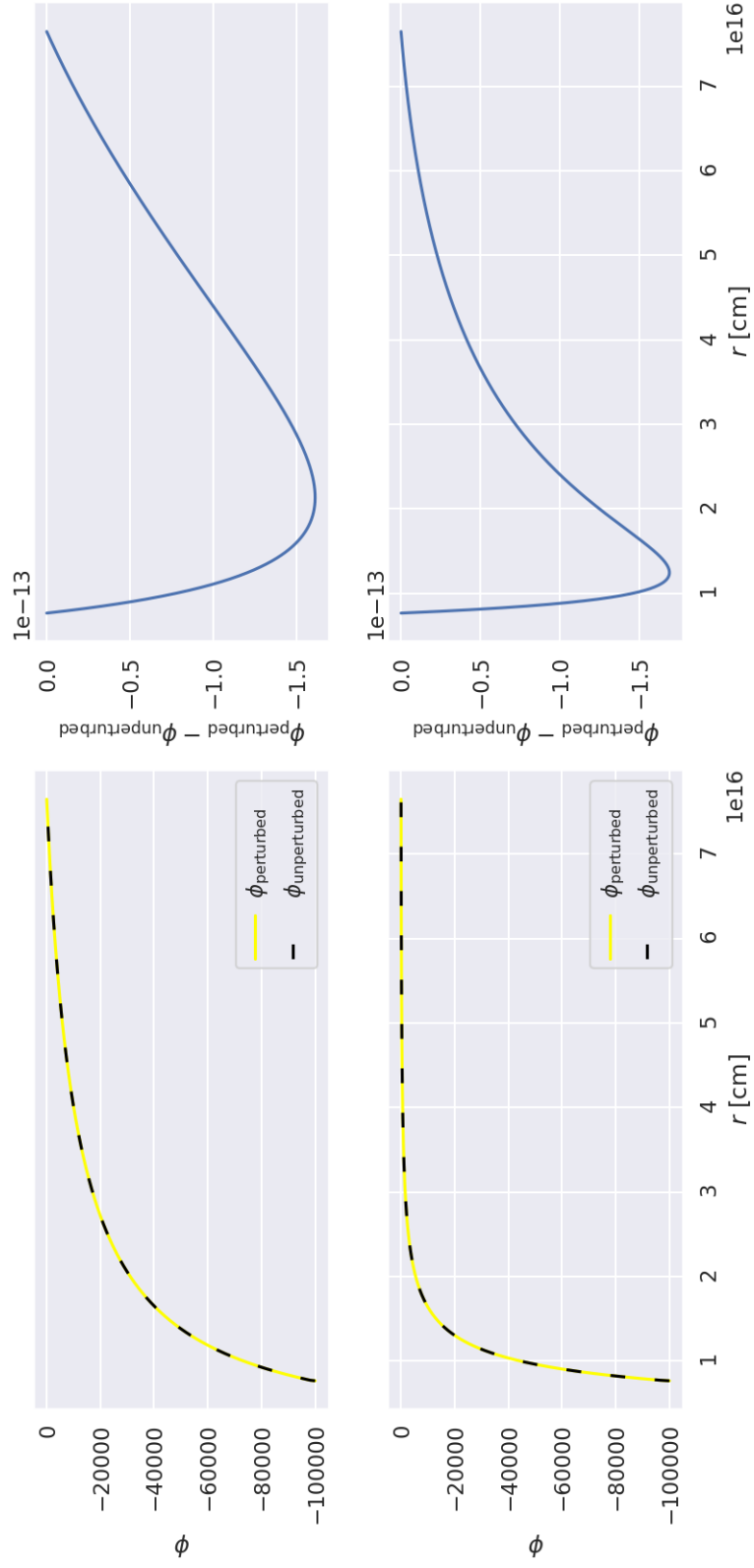


Figure 5.5: Numerical solution (distance to Voyager1 $\propto 150$ AU) – Spherical coordinates (top panel), Polar coordinates (bottom panel). Both calculations are carried out with the density profile $\rho = 0$.

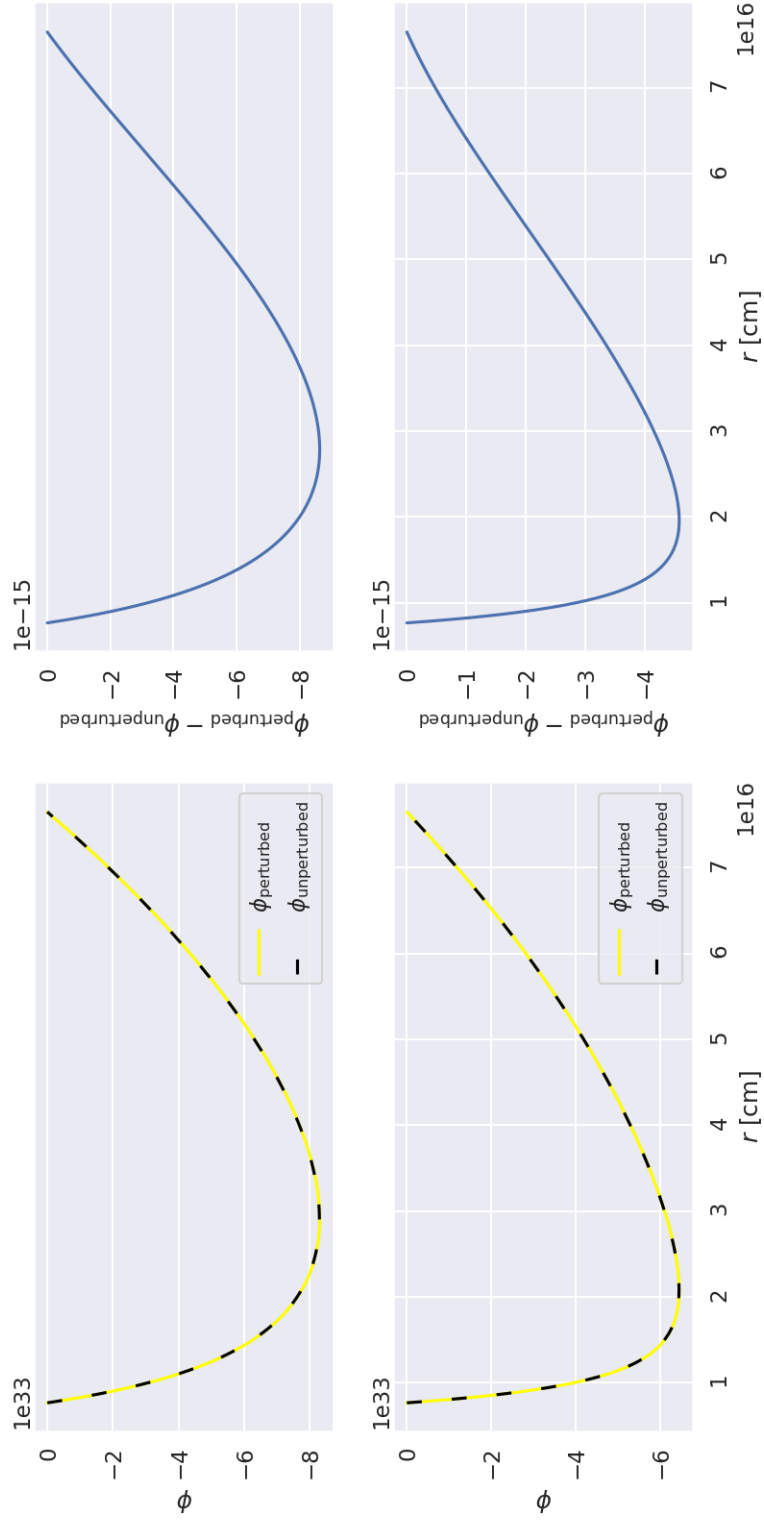


Figure 5.6: Numerical solution (distance to Voyager1 $\propto 150$ AU) – Spherical coordinates (top panel), Polar coordinates (bottom panel). Both calculations are carried out with the density profile $\rho \propto \text{const}$ ($\text{const} = 1$).

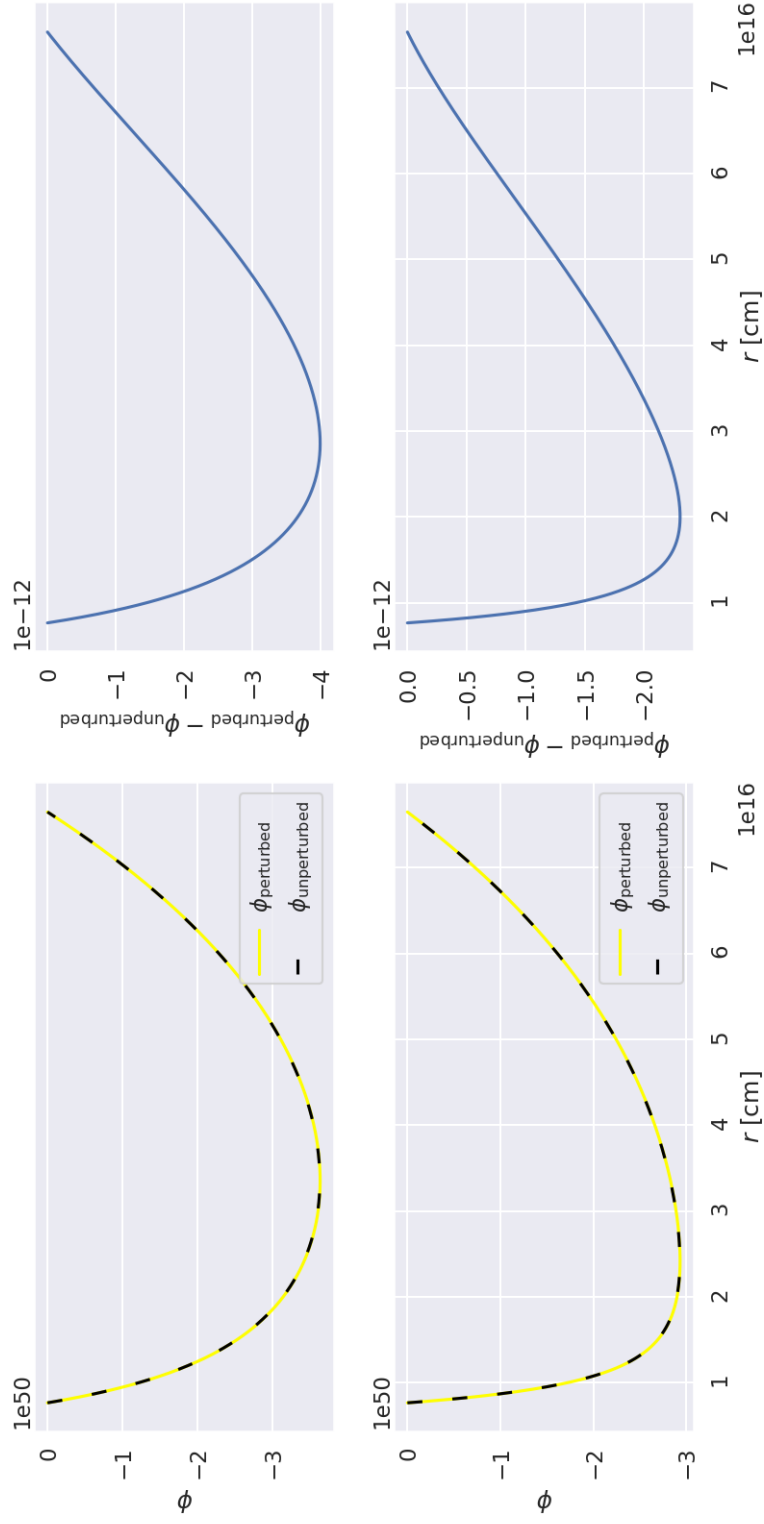


Figure 5.7: Numerical solution (distance to Voyager1 $\propto 150$ AU) – Spherical coordinates (top panel), Polar coordinates (bottom panel). Both calculations are carried out with the density profile $\rho \propto r$.

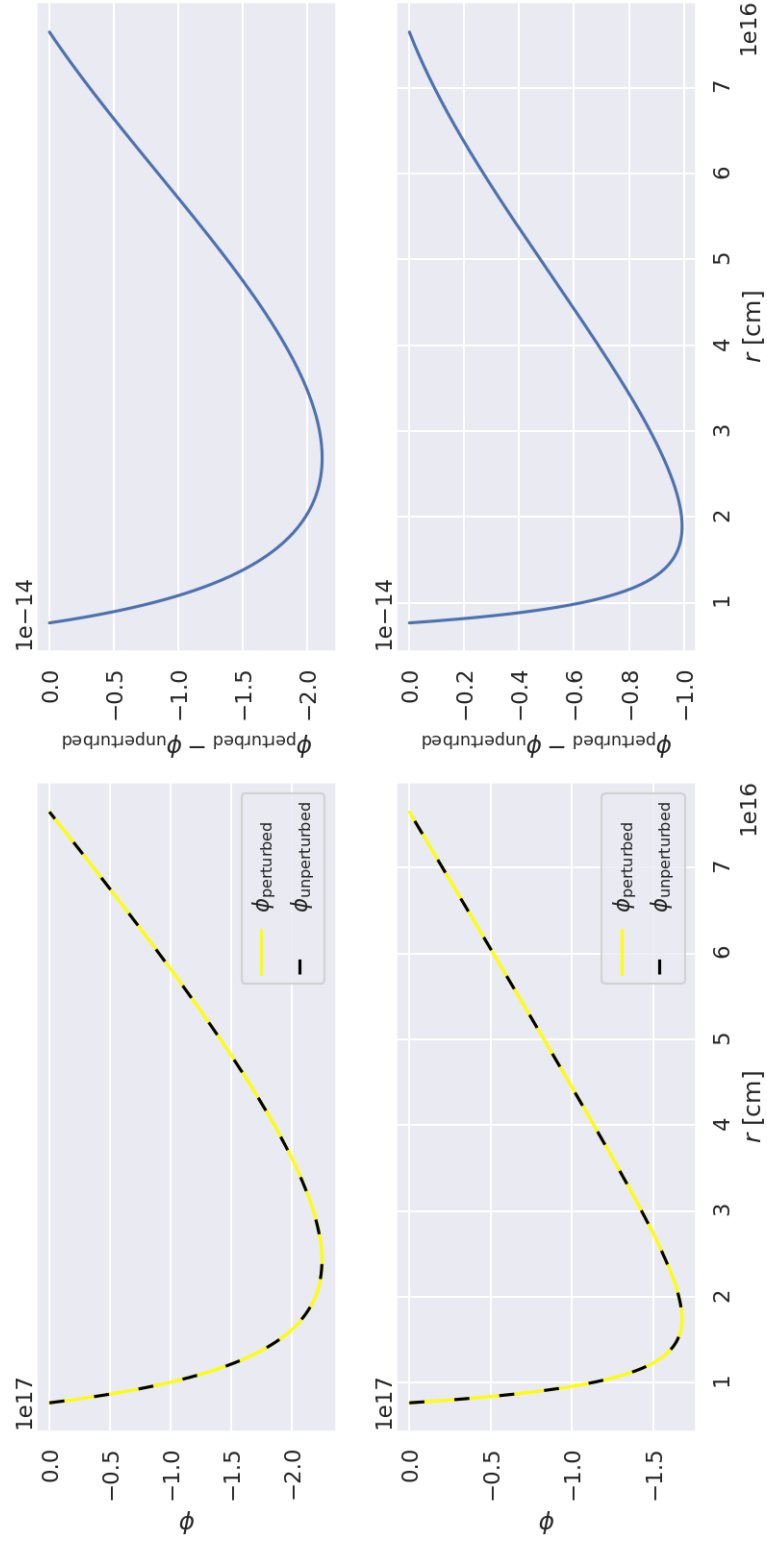


Figure 5.8: Numerical solution (distance to Voyager1 $\propto 150$ AU) – Spherical coordinates (top panel), Polar coordinates (bottom panel). Both calculations are carried out with the density profile $\rho \propto \frac{1}{r}$.

5.3 Distance of the gravitational interaction of the sun

For the distance of the gravitational interaction of the sun we also observe large deviation between $\phi_{\text{unperturbed}}$ and $\phi_{\text{perturbed}}$ in the case of zero density. For long distances, both potentials are close to zero, which are reasonable boundary conditions. Given the analytical solutions (5.1) and (5.2) we are able to determine the expected difference between the two potentials in the case of vacuum assuming spherical symmetry. The difference will be given by the leading term ($\sqrt{2\Lambda r}$) (same as for Sun-Jupiter distance), which for the distance 120 000 Au is at the level $\sim 10^{-10}$. The numerical method described in Chapter 4 above gives identical results for the selected case (see Figure 5.9).

After adding the mass to the problem, the difference between the calculated potentials is in some cases reduced by several orders of magnitude, but in the case of linearly increasing density with distance increases by one order of power (see Figure 5.11). In the case of constant density the potential difference shifts to the level of 10^{-12} (see Figure 5.10). For linearly decreasing density, the difference is at 10^{-11} (see Figure 5.12).

Given the choice of density profile we observe a considerable variable distribution of differences for the potentials $\phi_{\text{unperturbed}}$ and $\phi_{\text{perturbed}}$. However, this does not play a big role as even a difference of a few 10 000 Au at such a distance still accounts for a theoretically measurable difference in potential.

We do not observe a significant change in results given different choice of coordinates. However, changing the coordinate system causes a shift in the distance where the maximum difference between the calculated potentials takes place.

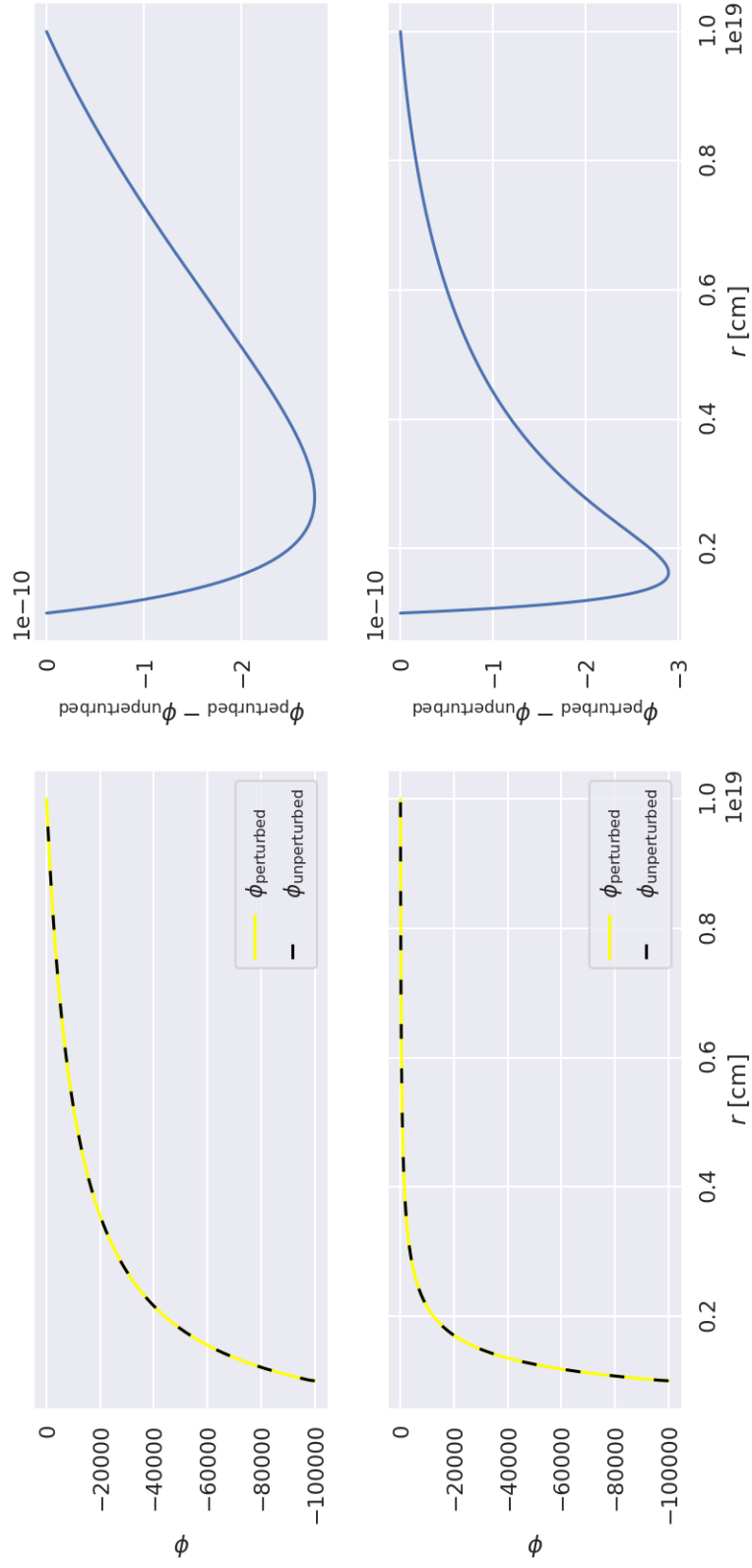


Figure 5.9: Numerical solution (radius of solar system $\propto 120\,000$ AU) – Spherical coordinates (top panel), Polar coordinates (bottom panel). Both calculations are carried out with the density profile $\rho = 0$.

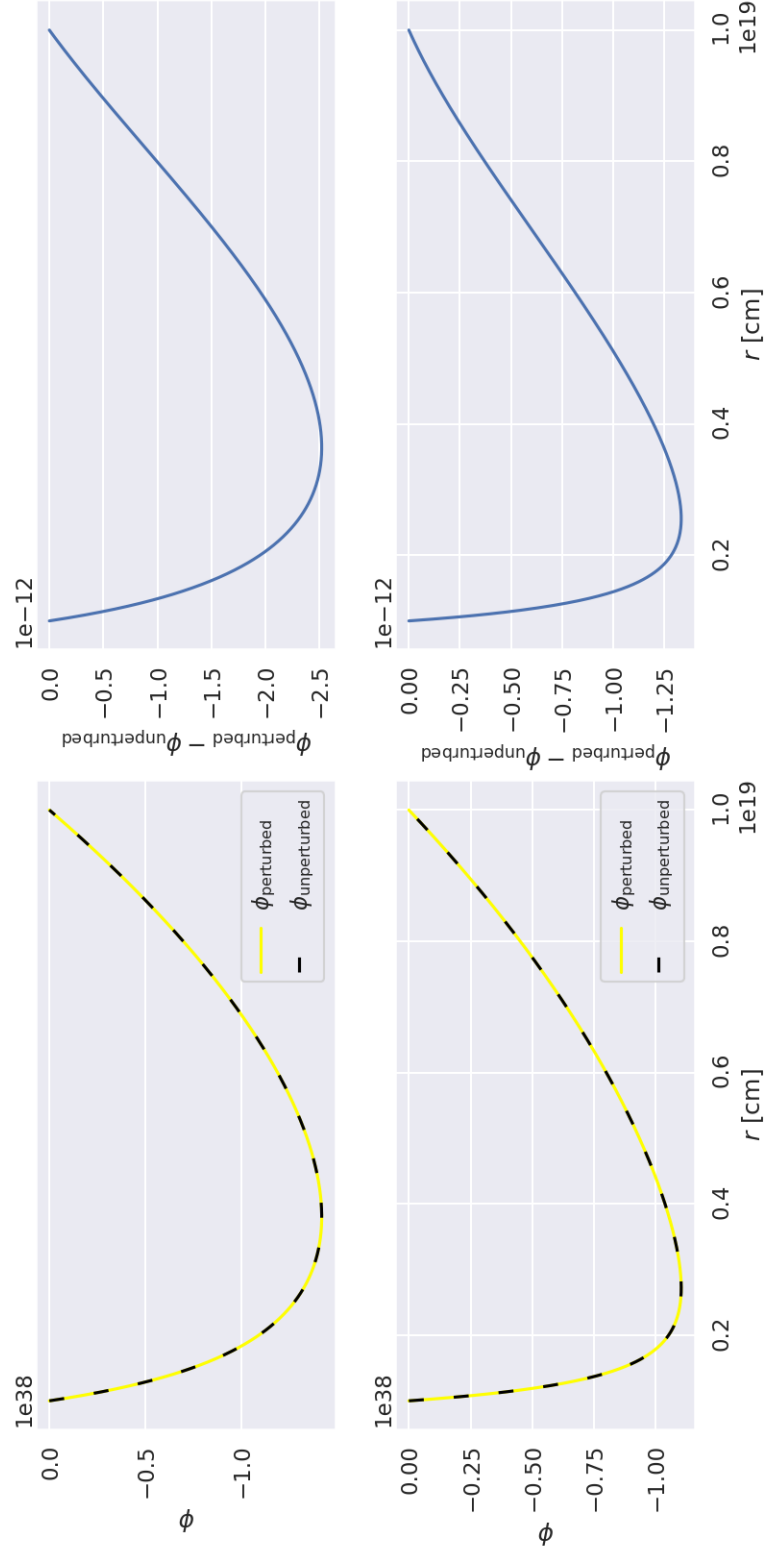


Figure 5.10: Numerical solution (radius of solar system $\propto 120\,000$ AU) – Spherical coordinates (top panel), Polar coordinates (bottom panel). Both calculations are carried out with the density profile $\rho \propto \text{const}$ ($\text{const} = 1$).

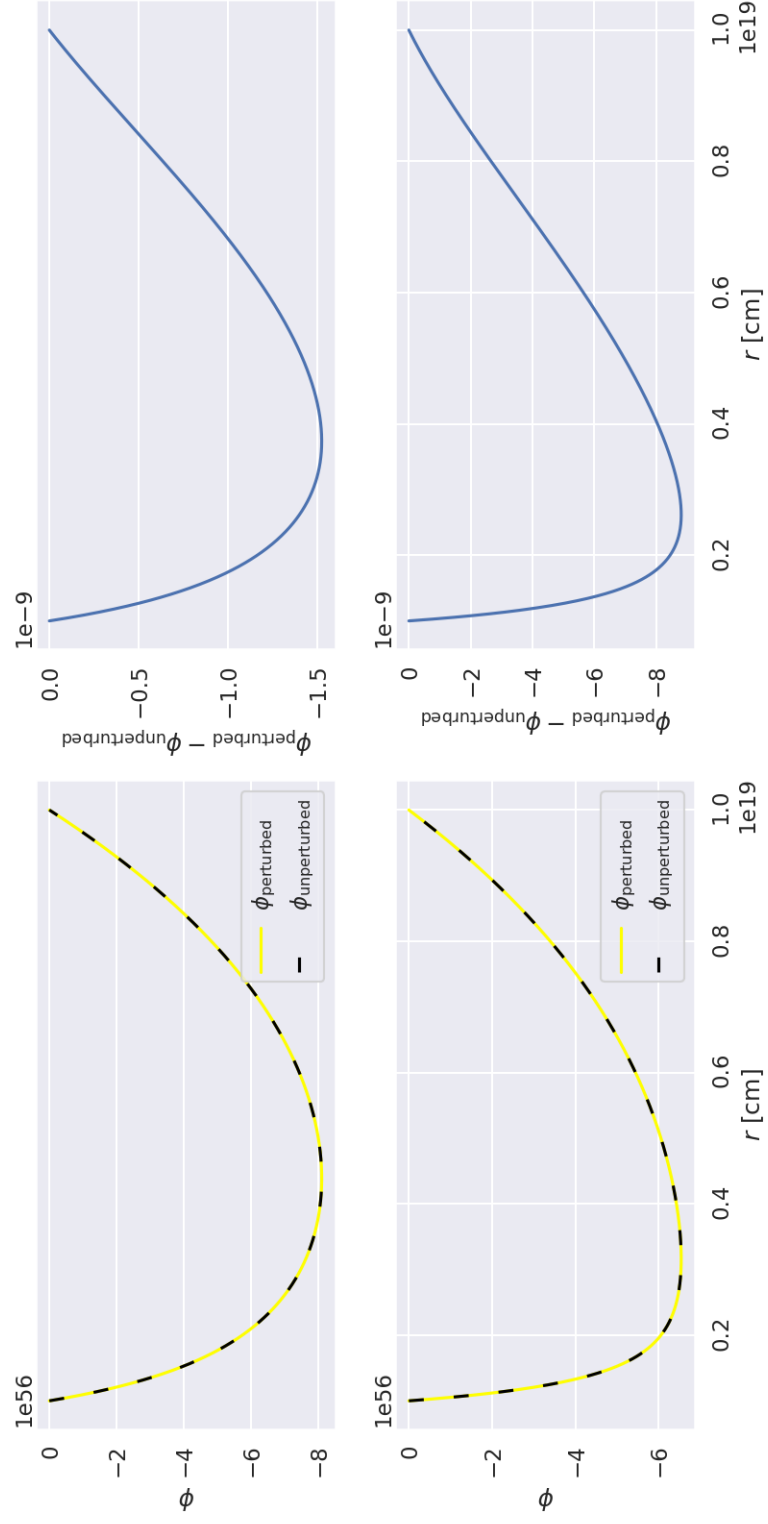


Figure 5.11: Numerical solution (radius of solar system $\propto 120\,000$ AU) – Spherical coordinates (top panel), Polar coordinates (bottom panel). Both calculations are carried out with the density profile $\rho \propto r$.

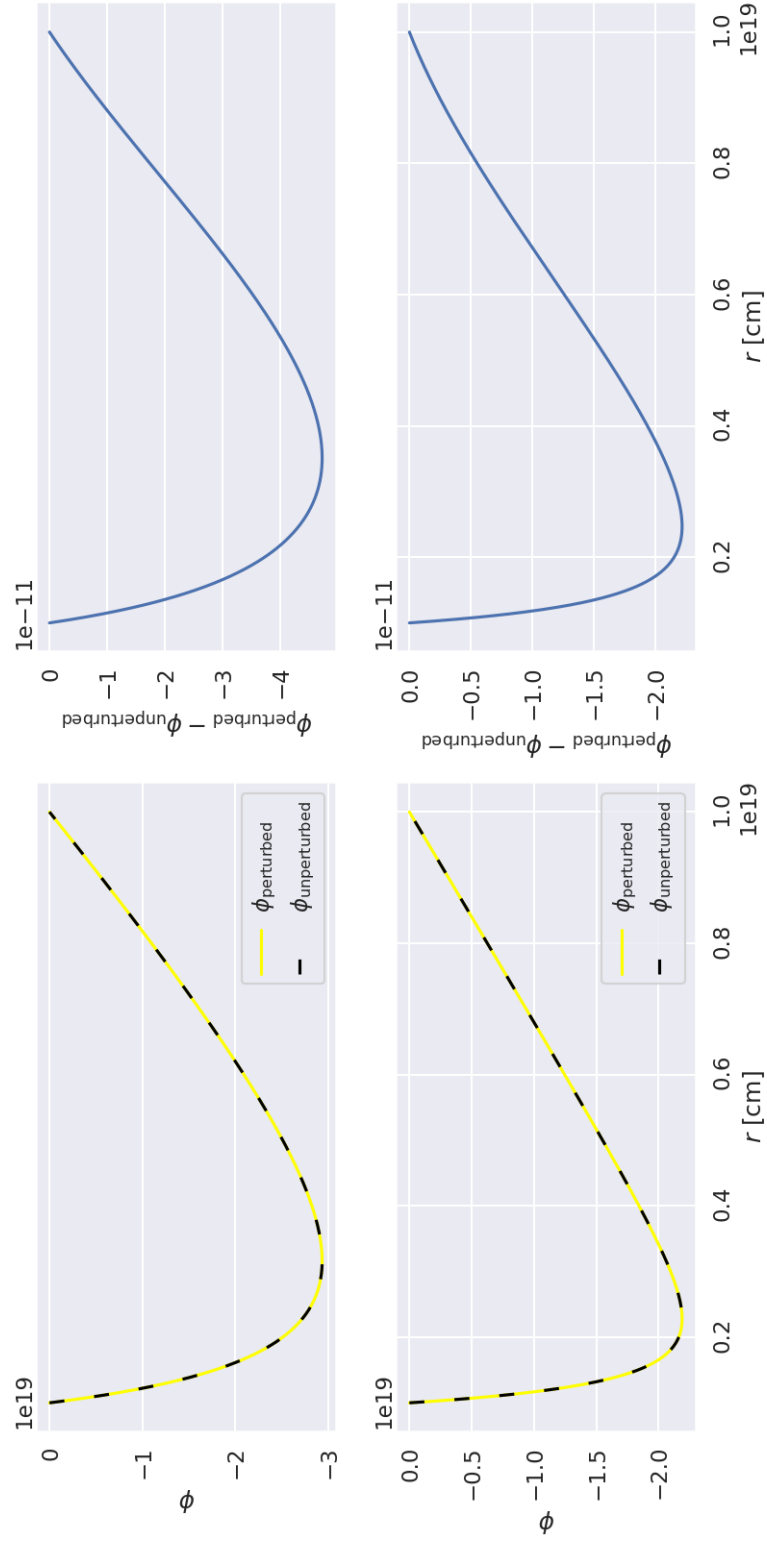


Figure 5.12: Numerical solution (radius of solar system $\propto 120\,000$ AU) – Spherical coordinates (top panel), Polar coordinates (bottom panel). Both calculations are carried out with the density profile $\rho \propto \frac{1}{r}$.

5.4 Distance of the radius of our galaxy

For the distance of the gravitational interaction on the scale of the radius of our galaxy, we observe deviation between $\phi_{\text{unperturbed}}$ and $\phi_{\text{perturbed}}$ in the case of zero density. For long distances, both potentials are close to zero, which are reasonable boundary conditions. Given the analytical solutions (5.1) and (5.2) we are able to determine the expected difference between the two potentials in the case of vacuum assuming spherical symmetry. The difference will be given by the leading term ($\sqrt{2\Lambda}r$) (same as for Sun-Jupiter distance), which for the distance 105 700 ly is at the level $\sim 10^{-5}$. The numerical method described in Chapter 4 above gives identical results for the selected case (see Figure 5.13).

After adding the mass to the problem, the difference between the calculated potentials is in some cases reduced by several orders of magnitude but in the case of linearly increasing density profile it increases by one order of power (see Figure 5.15). In the case of constant density the potential difference shifts to the level of 10^{-9} (see Figure 5.14). For linearly decreasing density, the difference is at 10^{-8} (see Figure 5.16).

We do not observe a significant change in results given different choice of coordinates. However, changing the coordinate system causes a shift in the distance where the maximum difference between the calculated potentials takes place.

Overall, the differences on such large scales should theoretically be detectable. In general the dimensions of galaxies in the universe vary as well as their density distribution, which will significantly change the order differences compared to the ones we calculated. However, given the galactic scales and the leading term ($\sqrt{2\Lambda}r$) of the series, we can state that the differences between $\phi_{\text{unperturbed}}$ and $\phi_{\text{perturbed}}$ will certainly be detectable for some cases.

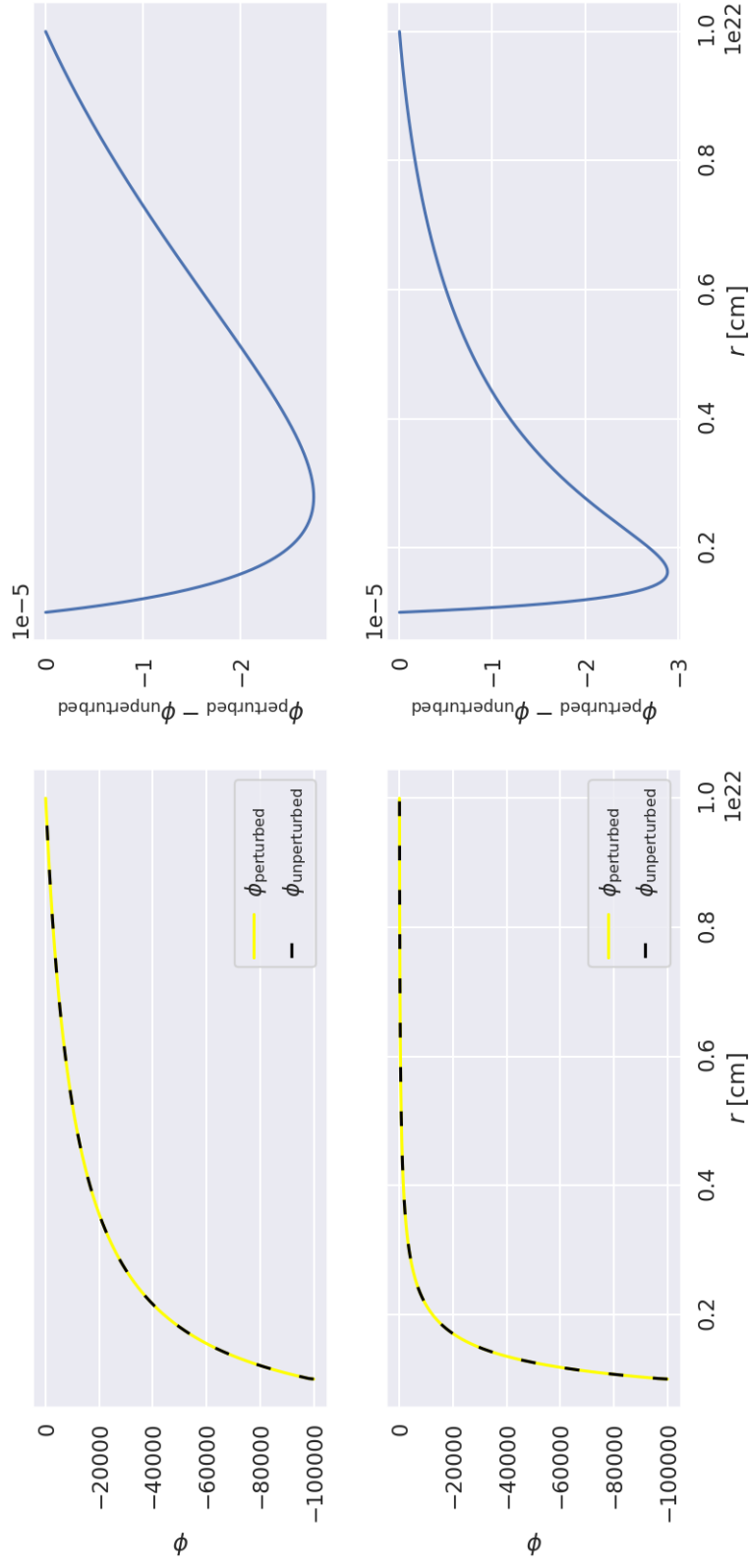


Figure 5.13: Numerical solution (radius of galaxy $\propto 105\,700$ ly) – Spherical coordinates (top panel), Polar coordinates (bottom panel). Both calculations are carried out with the density profile $\rho = 0$.

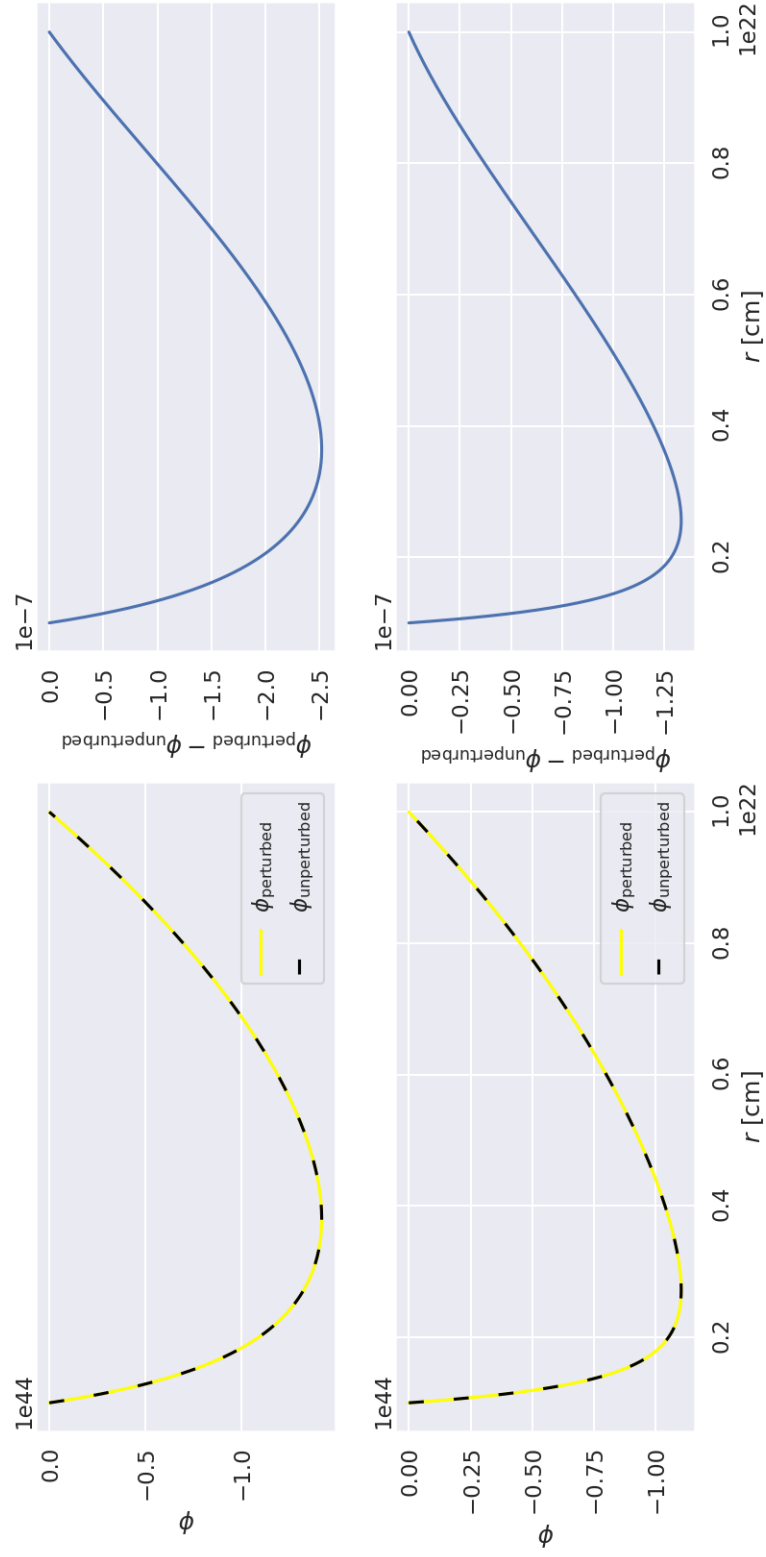


Figure 5.14: Numerical solution (radius of galaxy $\propto 105\,700$ ly) – Spherical coordinates (top panel), Polar coordinates (bottom panel). Both calculations are carried out with the density profile $\rho \propto \text{const}$ ($\text{const} = 1$).

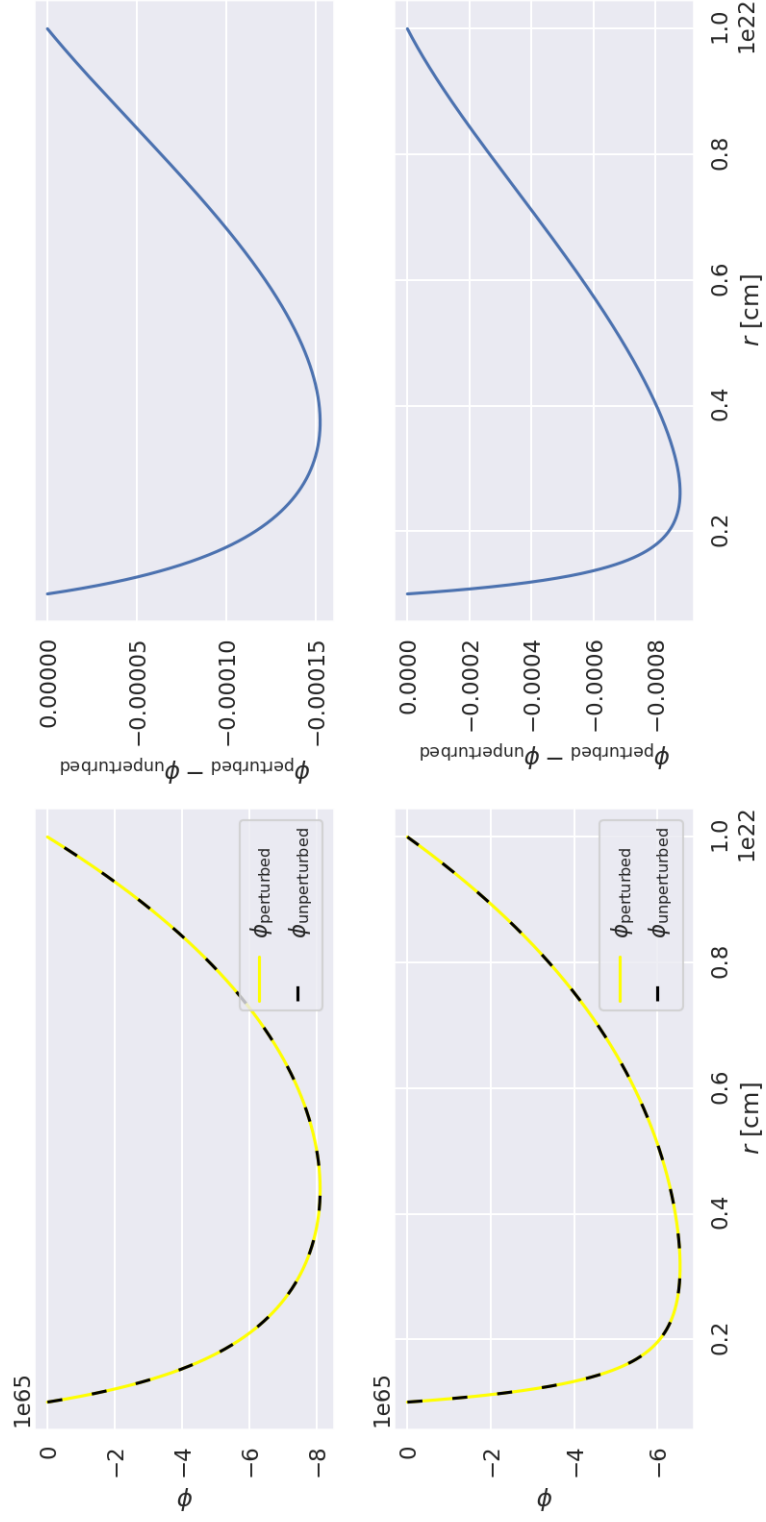


Figure 5.15: Numerical solution (radius of galaxy $\propto 10^5$ 700 ly) – Spherical coordinates (top panel), Polar coordinates (bottom panel). Both calculations are carried out with the density profile $\rho \propto r$.

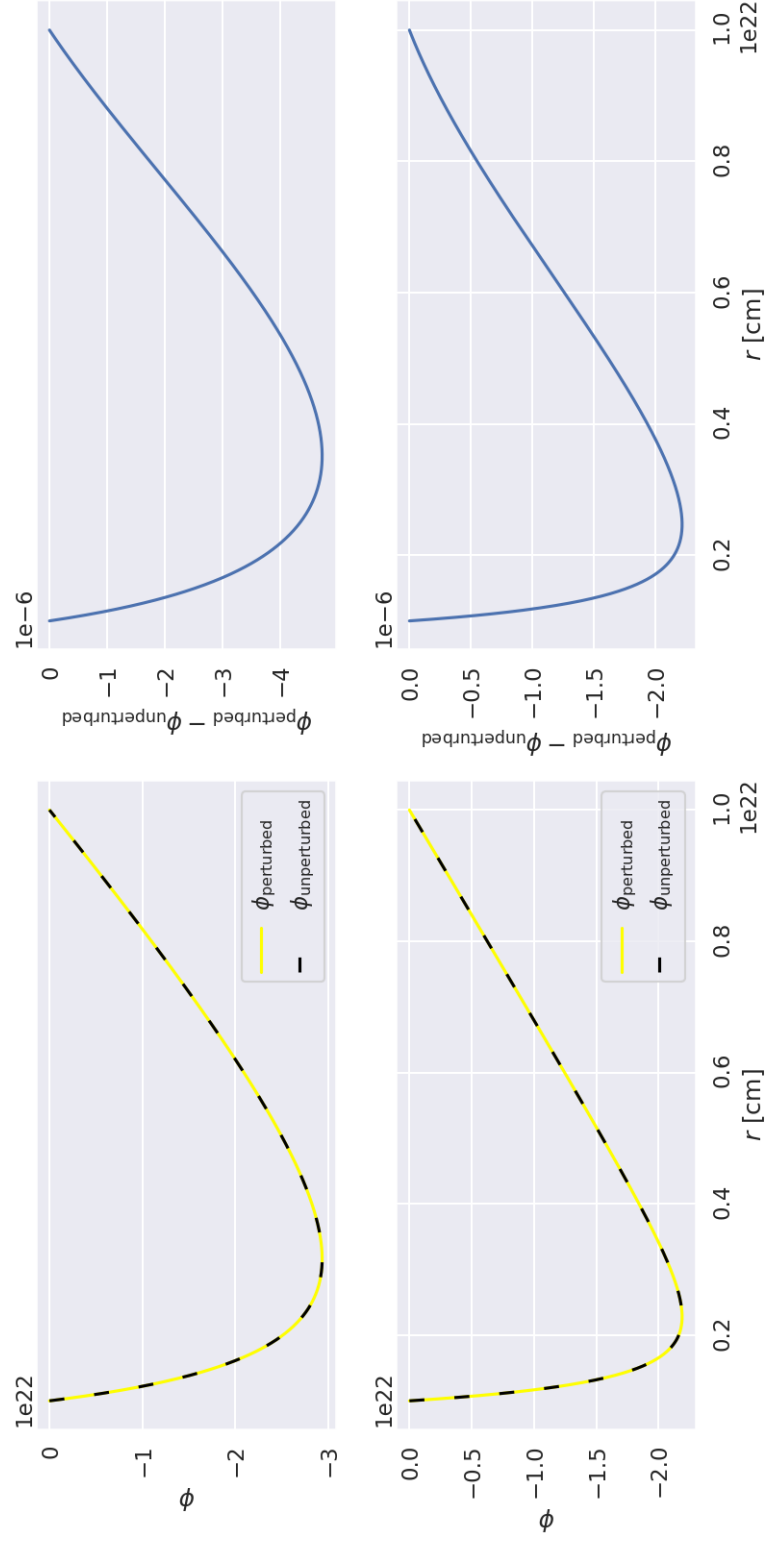


Figure 5.16: Numerical solution (radius of galaxy $\propto 105\,700$ ly) – Spherical coordinates (top panel), Polar coordinates (bottom panel). Both calculations are carried out with the density profile $\rho \propto \frac{1}{r}$.

5.5 Commentary on the numerical solutions

The numerical method we used to determine the difference between $\phi_{\text{unperturbed}}$ and $\phi_{\text{perturbed}}$ was implemented for four different density profiles, i.e. $\rho = 0$, $\rho = \text{const}$, $\rho \propto r$ and $\rho \propto \frac{1}{r}$. We compared the accuracy of the numerical solution with the exact analytical solution for one density profile, specifically for $\rho = 0$.

The theoretical basis for the numerical solution of such a system is applicable to various input parameters of the mass distribution on the studied scales. The calculations were performed, only on spatial scales up to $\sim 10^{23}$.

We show all captured differences for the considered density profiles in both coordinate systems.

Table 5.1: The difference between $\phi_{\text{unperturbed}}$ and $\phi_{\text{perturbed}}$ for different density profiles, i.e. $\rho = 0$, $\rho = \text{const}$, $\rho \propto r$ and $\rho \propto \frac{1}{r}$.

	Distance [cm]	$\rho = 0$	$\rho = \text{const}$	$\rho \propto \frac{1}{r}$	$\rho \propto r$
Spherical coordinates	7.8×10^{13}	10^{-14}	10^{-16}	10^{-15}	10^{-13}
	2.2×10^{15}	10^{-13}	10^{-15}	10^{-14}	10^{-12}
	1.8×10^{18}	10^{-10}	10^{-12}	10^{-11}	10^{-9}
	1.0×10^{23}	10^{-5}	10^{-7}	10^{-6}	10^{-4}
Polar coordinates	7.8×10^{13}	10^{-14}	10^{-16}	10^{-15}	10^{-13}
	2.2×10^{15}	10^{-13}	10^{-15}	10^{-14}	10^{-12}
	1.8×10^{18}	10^{-10}	10^{-12}	10^{-11}	10^{-9}
	1.0×10^{23}	10^{-5}	10^{-7}	10^{-6}	10^{-4}

Due to the double precision, we see that the differences between $\phi_{\text{unperturbed}}$ and $\phi_{\text{perturbed}}$ on the spatial scales up to the size of the Sun-Jupiter distance are detectable. The order of magnitude of differences with respect to the density profiles used may be even greater if we approach the real density distribution. We expect the real density profile to reduce the vacuum error by one to two orders of magnitude, bringing us closer to the limit value 10^{-16} . It is not certain with regard to today's instruments whether it is possible to observe such minimal differences in the Keplerian orbits given the perturbation Λ -term. At smaller distances than the Sun-Jupiter distance, the difference $\phi_{\text{unperturbed}}$ and $\phi_{\text{perturbed}}$ is likely to be immeasurable due to reaching the limit of the double precision.

Conclusion and future prospectives

In the introduction part we have highlighted the most important milestones of the cosmological constant Λ . We have also shown that the existence of Λ in Einstein's field equations follows directly and relentlessly from the basic principles the general relativity is built upon.

Another extensive part of this work was the derivation of the Newtonian limit from Einstein's field equations. We then used the Poisson's equation of Newtonian gravity and the modified Poisson's equation of the Newtonian limits of Einstein's field equations as starting equations to account for the differences in potential once we introduced the cosmological constant Λ .

After introducing spherical and polar symmetry, we have numerically calculated the difference in potentials of both equations for specified density profiles ($\rho = 0$, $\rho \propto \text{const}$ ($\text{const} = 1$), $\rho \propto r$, $\rho \propto \frac{1}{r}$). We derived an analytical solution for zero density, based on which we checked the correctness of the numerical solution.

We show different behaviour of $\phi_{\text{unperturbed}}$ and $\phi_{\text{perturbed}}$ at different distances (5 Au – 100 000 ly), for four density profiles ($\rho = 0$, $\rho \propto \text{const}$ ($\text{const} = 1$), $\rho \propto r$, $\rho \propto \frac{1}{r}$) in two coordinate systems (Spherical coordinates, Polar coordinates). At these distances the order of the magnitude of the differences between $\phi_{\text{unperturbed}}$ and $\phi_{\text{perturbed}}$ is ranging from 10^{-17} to 10^{-4} depending on the density profile (see Figures (5.1)-(5.16) and table (5.1)). The difference between $\phi_{\text{unperturbed}}$ and $\phi_{\text{perturbed}}$ decreases with distance according to the theoretical assumptions.

The thesis also opens many future prospects, which can be summarized as follows

- To describe the most realistic density profiles for each distance scale. Based on these data, then to determine the realistic distance at which the influence of the cosmological constant Λ can be observed.
- To create a theoretical model that could measure the cosmological constant Λ on such small scales.
- To propose an experimental solution to the problem based on a theoretical model.

Bibliography

- R. J. Adler, B. Casey, and O. C. Jacob. Vacuum catastrophe: An elementary exposition of the cosmological constant problem. *American Journal of Physics*, 63(7):620–626, July 1995. doi: 10.1119/1.17850.
- D. Anadijiban. *The Special Theory of Relativity A Mathematical Exposition / by Anadijiban Das*. Universitext. Springer New York : Imprint: Springer, New York, NY, 1st ed. 1993. edition, 1993. ISBN 0-387-94042-1.
- M. Apostol. *Calculus*. 2nd edition. Wiley, 1967.
- J. C. Baker, Keith Grainge, M. P. Hobson, Michael E. Jones, R. Kneissl, A. N. Lasenby, C. M. M. O’Sullivan, Guy Pooley, G. Rocha, Richard Saunders, P. F. Scott, and E. M. Waldram. Detection of cosmic microwave background structure in a second field with the Cosmic Anisotropy Telescope. *Monthly Notices of the Royal Astronomical Society*, 308(4):1173–1178, 10 1999. ISSN 0035-8711. doi: 10.1046/j.1365-8711.1999.02829.x. URL <https://doi.org/10.1046/j.1365-8711.1999.02829.x>.
- S. M. Carroll, William H. Press, and Edwin L. Turner. The Cosmological Constant. *Annual Review of Astronomy and Astrophysics*, 30(1):499–542, 1992. doi: 10.1146/annurev.aa.30.090192.002435. URL <https://doi.org/10.1146/annurev.aa.30.090192.002435>.
- J. Coffey. How Big Is The Milky Way, 2010. URL <https://web.archive.org/web/20160502182323/http://www.universetoday.com/75691/how-big-is-the-milky-way/>.
- J. Earman. Lambda: The Constant That Refuses to Die. *Archive for History of Exact Sciences*, 55(3):189–220, 2001. ISSN 00039519, 14320657. URL <http://www.jstor.org/stable/41134106>.
- A. Einstein. Die Feldgleichungen der Gravitation. *Sitzungsberichte der Königlich Preußischen Akademie der Wissenschaften (Berlin)*, pages 844–847, January 1915.
- A. Einstein. Die Grundlage der allgemeinen Relativitätstheorie. *Annalen der Physik*, 354(7):769–822, 1916. doi: <https://doi.org/10.1002/andp.19163540702>. URL <https://onlinelibrary.wiley.com/doi/abs/10.1002/andp.19163540702>.
- A. Einstein. Kosmologische Betrachtungen zur allgemeinen Relativitätstheorie. *Sitzungsberichte der Königlich Preußischen Akademie der Wissenschaften (Berlin)*, pages 142–152, January 1917.
- A. Einstein. *Zum kosmologischen Problem der allgemeinen Relativitätstheorie*, volume 96, pages 361–364. 08 2006. ISBN 9783527608959. doi: 10.1002/3527608958.ch43.
- A. Friedmann. Über die Krümmung des Raumes. *Zeitschrift für Physik*, 10: 377–386, January 1922. doi: 10.1007/BF01332580.

- G. Gamow. The Evolutionary Universe. *Scientific American*, 195(3):136–156, September 1956. doi: 10.1038/scientificamerican0956-136.
- J. Hartle. *Gravity: An Introduction to Einstein’s General Relativity*. 1st edition. Pearson, 2002.
- E. Hubble. A relation between distance and radial velocity among extra-galactic nebulae. *Proceedings of the National Academy of Sciences*, 15(3):168–173, 1929. ISSN 0027-8424. doi: 10.1073/pnas.15.3.168. URL <https://www.pnas.org/content/15/3/168>.
- CH. Kohn. A Solution to the Cosmological Constant Problem in Two Time Dimensions. *Journal of High Energy Physics, Gravitation and Cosmology*, 6(4):640–655, 2020. doi: 10.4236/jhepgc.2020.64043.
- L. D. Landau and E. M. Lifshitz. *The Classical Theory of Fields*. Butterworth-Heinemann, 4 edition, January 1980. ISBN 0750627689. URL <http://www.worldcat.org/isbn/0750627689>.
- G. Lemaître. Un Univers homogène de masse constante et de rayon croissant rendant compte de la vitesse radiale des nébuleuses extra-galactiques. *Annales de la Société Scientifique de Bruxelles*, 47:49–59, January 1927.
- M. Livio. Brilliant Blunders: From Darwin to Einstein—Colossal Mistakes by Great Scientists That Changed Our Understanding of Life and the Universe. *Physics Today*, 66(8):48, 2013. doi: <https://doi.org/10.1063/PT.3.2084>.
- Ch. W. Misner, K. S. Thorne, and J. A. Wheeler. *Gravitation*. W. H. Freeman, San Francisco, 1973. ISBN 978-0-7167-0344-0, 978-0-691-17779-3.
- S. Nasa. Jupiter, 2021a. URL <https://solarsystem.nasa.gov/planets/jupiter/overview/>.
- S. Nasa. Voyager I, 2021b. URL <https://voyager.jpl.nasa.gov/mission/status/>.
- S. Nasa. Oort Cloud, 2021c. URL <https://solarsystem.nasa.gov/solar-system/oort-cloud/overview/>.
- M. Nowakowski. The Consistent Newtonian Limit of Einstein’s Gravity with a Cosmological Constant. *International Journal of Modern Physics D*, 10(05):649–661, Oct 2001. ISSN 1793-6594. doi: 10.1142/s0218271801001189. URL <http://dx.doi.org/10.1142/S0218271801001189>.
- S. Perlmutter, P. Press, and L. Yarris. Science Magazine Names Supernova Cosmology Project ”Breakthrough of the Year”. *research News*, 1998. URL <https://www2.lbl.gov/supernova/>.
- S. Perlmutter, G. Aldering, G. Goldhaber, R. A. Knop, P. Nugent, P. G. Castro, S. Deustua, S. Fabbro, A. Goobar, D. E. Groom, I. M. Hook, A. G. Kim, M. Y. Kim, J. C. Lee, N. J. Nunes, R. Pain, C. R. Pennypacker, R. Quimby, C. Lidman, R. S. Ellis, M. Irwin, R. G. McMahon, P. Ruiz-Lapuente, N. Walton, B. Schaefer, B. J. Boyle, A. V. Filippenko, T. Matheson, A. S. Fruchter,

- N. Panagia, H. J. M. Newberg, W. J. Couch, and The Supernova Cosmology Project. Measurements of Ω and Λ from 42 high-redshift supernovae. *The Astrophysical Journal*, 517(2):565–586, jun 1999. doi: 10.1086/307221. URL <https://doi.org/10.1086/307221>.
- A. G. Riess, A. V. Filippenko, Peter Challis, Alejandro Clocchiatti, Alan Diercks, Peter M. Garnavich, Ron L. Gilliland, Craig J. Hogan, Saurabh Jha, Robert P. Kirshner, B. Leibundgut, M. M. Phillips, David Reiss, Brian P. Schmidt, Robert A. Schommer, R. Chris Smith, J. Spyromilio, Christopher Stubbs, Nicholas B. Suntzeff, and John Tonry. Observational Evidence from Supernovae for an Accelerating Universe and a Cosmological Constant. *The Astronomical Journal*, 116(3):1009–1038, sep 1998. doi: 10.1086/300499. URL <https://doi.org/10.1086/300499>.
- S.E. Rugh and H. Zinkernagel. The quantum vacuum and the cosmological constant problem. *Studies in History and Philosophy of Science Part B: Studies in History and Philosophy of Modern Physics*, 33(4):663–705, 2002. ISSN 1355-2198. doi: [https://doi.org/10.1016/S1355-2198\(02\)00033-3](https://doi.org/10.1016/S1355-2198(02)00033-3). URL <https://www.sciencedirect.com/science/article/pii/S1355219802000333>.
- V. M. Slipher. Nebulae. *Proceedings of the American Philosophical Society*, 56: 403–409, January 1917.
- M. Tavora. A Heuristic Derivation of Einstein’s Gravity Equations. 2020. URL <https://towardsdatascience.com/>.
- S. Walters. How Einstein Got His Field Equations, 2016.
- S. Weinberg. The cosmological constant problem. *Rev. Mod. Phys.*, 61:1–23, Jan 1989. doi: 10.1103/RevModPhys.61.1. URL <https://link.aps.org/doi/10.1103/RevModPhys.61.1>.
- M.D. Weir, R.L. Finney, and G.B. Thomas. *Calculus and Analytic Geometry (9th Edition)*. 9th edition. Addison Wesley, 1996.
- H. Yukawa. On the Interaction of Elementary Particles I. *Proc. Phys. Math. Soc. Jap.*, 17:48–57, 1935. doi: 10.1143/PTPS.1.1.

List of Figures

5.1	Numerical solution (distance Sun to Jupiter $\propto 5$ AU) – Spherical coordinates (top panel), Polar coordinates (bottom panel). Both calculations are carried out with the density profile $\rho = 0$	29
5.2	Numerical solution (distance Sun to Jupiter $\propto 5$ AU) – Spherical coordinates (top panel), Polar coordinates (bottom panel). Both calculations are carried out with the density profile $\rho \propto const$ ($const = 1$).	30
5.3	Numerical solution (distance Sun to Jupiter $\propto 5$ AU) – Spherical coordinates (top panel), Polar coordinates (bottom panel). Both calculations are carried out with the density profile $\rho \propto r$	31
5.4	Numerical solution (distance Sun to Jupiter $\propto 5$ AU) – Spherical coordinates (top panel), Polar coordinates (bottom panel). Both calculations are carried out with the density profile $\rho \propto \frac{1}{r}$	32
5.5	Numerical solution (distance to Voyager1 $\propto 150$ AU) – Spherical coordinates (top panel), Polar coordinates (bottom panel). Both calculations are carried out with the density profile $\rho = 0$	34
5.6	Numerical solution (distance to Voyager1 $\propto 150$ AU) – Spherical coordinates (top panel), Polar coordinates (bottom panel). Both calculations are carried out with the density profile $\rho \propto const$ ($const = 1$).	35
5.7	Numerical solution (distance to Voyager1 $\propto 150$ AU) – Spherical coordinates (top panel), Polar coordinates (bottom panel). Both calculations are carried out with the density profile $\rho \propto r$	36
5.8	Numerical solution (distance to Voyager1 $\propto 150$ AU) – Spherical coordinates (top panel), Polar coordinates (bottom panel). Both calculations are carried out with the density profile $\rho \propto \frac{1}{r}$	37
5.9	Numerical solution (radius of solar system $\propto 120\,000$ AU) – Spherical coordinates (top panel), Polar coordinates (bottom panel). Both calculations are carried out with the density profile $\rho = 0$	39
5.10	Numerical solution (radius of solar system $\propto 120\,000$ AU) – Spherical coordinates (top panel), Polar coordinates (bottom panel). Both calculations are carried out with the density profile $\rho \propto const$ ($const = 1$).	40
5.11	Numerical solution (radius of solar system $\propto 120\,000$ AU) – Spherical coordinates (top panel), Polar coordinates (bottom panel). Both calculations are carried out with the density profile $\rho \propto r$	41
5.12	Numerical solution (radius of solar system $\propto 120\,000$ AU) – Spherical coordinates (top panel), Polar coordinates (bottom panel). Both calculations are carried out with the density profile $\rho \propto \frac{1}{r}$	42
5.13	Numerical solution (radius of galaxy $\propto 105\,700$ ly) – Spherical coordinates (top panel), Polar coordinates (bottom panel). Both calculations are carried out with the density profile $\rho = 0$	44

5.14	Numerical solution (radius of galaxy $\propto 105\,700$ ly) – Spherical coordinates (top panel), Polar coordinates (bottom panel). Both calculations are carried out with the density profile $\rho \propto \text{const}$ ($\text{const} = 1$)	45
5.15	Numerical solution (radius of galaxy $\propto 105\,700$ ly) – Spherical coordinates (top panel), Polar coordinates (bottom panel). Both calculations are carried out with the density profile $\rho \propto r$	46
5.16	Numerical solution (radius of galaxy $\propto 105\,700$ ly) – Spherical coordinates (top panel), Polar coordinates (bottom panel). Both calculations are carried out with the density profile $\rho \propto \frac{1}{r}$	47

List of Tables

5.1	The difference between $\phi_{\text{unperturbed}}$ and $\phi_{\text{perturbed}}$ for different density profiles, i.e. $\rho = 0$, $\rho = \text{const}$, $\rho \propto r$ and $\rho \propto \frac{1}{r}$	48
-----	--	----

List of Abbreviations

NL - Newtonian limit

EE - Einstein's equations

A. Analytical solution and Taylor series

A.1 Analytical solution of the Newtonian limit for vacuum

Consider a vacuum where the density is zero. We will rewrite equation (3.37) in the form:

$$\Delta\phi + 2\Lambda\phi = -\Lambda. \quad (\text{A.1})$$

In spherical symmetry, a partial differential equation (A.1) transitions to an ordinary differential equation. Let us first solve the homogeneous part, i.e. the right side is equal to zero. Let us consider a similar differential equation with the opposite sign, i.e. $\Delta\phi - 2\Lambda\phi = -\Lambda$, with its homogeneous part is $\Delta\phi - 2\Lambda\phi = 0$. This latter type of differential equation was already solved by Hideki Yukawa in 1934, so let us assume that the solution of homogeneous part of equation (A.1) will be in the form $\phi(r) = \frac{A}{r}\cos(Br) + \frac{C}{r}\sin(Br)$. However, since our equation for the case of vacuum is different in the sign on the left hand side compared to the original Yukawa equation¹ [Yukawa, 1935], we consider the solution imaginary in exponential, i.e. a combination of sine and cosine functions. We will be interested in the constant B

$$\begin{aligned} & \frac{1}{r^2} \frac{d}{dr} \left(r^2 \frac{d}{dr} \right) \phi(r) + 2\Lambda\phi(r) = 0 \\ & \frac{1}{r^2} \frac{d}{dr} \left(r^2 \frac{d}{dr} \right) \left(\frac{A}{r}\cos(Br) + \frac{C}{r}\sin(Br) \right) + \\ & \quad + 2\Lambda \left(\frac{A}{r}\cos(Br) + \frac{C}{r}\sin(Br) \right) = 0 \\ & \frac{1}{r^2} \frac{d}{dr} \left(\cancel{r^2} \left[\frac{-AB\sin(Br)r - A\cos(Br) + CB\cos(Br)r - C\sin(Br)}{\cancel{r^2}} \right] \right) + \\ & \quad + 2\Lambda \left(\frac{A}{r}\cos(Br) + \frac{C}{r}\sin(Br) \right) = 0 \\ & \frac{1}{r^2} \left(-AB^2\cos(Br)r - \cancel{AB\sin(Br)} + \cancel{AB\sin(Br)} - CB^2\sin(Br)r + \right. \\ & \quad \left. + \cancel{CB\cos(Br)} - \cancel{CB\cos(Br)} + 2\Lambda \left(\frac{A}{r}\cos(Br) + \frac{C}{r}\sin(Br) \right) \right) = 0 \\ & -\frac{AB^2}{r}\cos(Br) - \frac{CB^2}{r}\sin(Br) + 2\Lambda \left(\frac{A}{r}\cos(Br) + \frac{C}{r}\sin(Br) \right) = 0 \\ & \quad \left(-AB^2 + 2\Lambda A \right) \cos(Br) + \left(-CB^2 + 2\Lambda C \right) \sin(Br) = 0. \end{aligned} \quad (\text{A.2})$$

¹The vacuum case of the Yukawa equation in Spherical coordinates is $(\Delta - \frac{1}{c^2} \frac{\partial^2}{\partial t^2} - \lambda^2)U = 0$, where the unknown potential U is a function of x, y, z a t [Yukawa, 1935].

Fulfilling the zero right hand side will lead to these combinations

$$\begin{aligned}
(-AB^2 + 2\Lambda A) = 0 \wedge (-CB^2 + 2\Lambda C) = 0 \vee \\
(-AB^2 + 2\Lambda A) = 0 \wedge \sin(Br) = 0 \vee \\
\cos(Br) = 0 \wedge (-CB^2 + 2\Lambda C) = 0 \vee \\
\cos(Br) = 0 \wedge \sin(Br) = 0.
\end{aligned} \tag{A.3}$$

From the above conditions (A.3) it is clear that only the first one can be met, because $\sin(r) = 0$ for $r = 0 + k\pi$, where $k \in \mathbf{N}$ and $\cos(r) = 0$ for $r = k\frac{\pi}{2}$, where $k \in \mathbf{N}$. Due to this, it is not possible to meet the fourth condition and resetting the parentheses is not possible for $r = 0 + k\pi$ or $r = k\frac{\pi}{2}$, so we are left with

$$(-AB^2 + 2\Lambda A) = 0 \wedge (-CB^2 + 2\Lambda C) = 0 \implies B = \pm\sqrt{2\Lambda}. \tag{A.4}$$

We consider the boundary condition for the potential at infinity to be zero. Since we considered only a real solution, we hide the resulting sign B in the appropriate constants A and C , which we denote as \bar{A} and \bar{C} . The analytical solution of the homogeneous part of the differential equation (A.1) then follows

$$\phi_0(r) = \frac{\bar{A}}{r} \cos\sqrt{2\Lambda}r + \frac{\bar{C}}{r} \sin\sqrt{2\Lambda}r. \tag{A.5}$$

We seek the particular solution with respect to the right side as a constant k

$$\phi_p(r) = k \tag{A.6}$$

and we estimate the value of constant k as

$$\begin{aligned}
\frac{1}{r^2} \frac{d}{dr} \left(r^2 \frac{d}{dr} \right) \phi_p(r) + 2\Lambda \phi_p(r) &= -\Lambda \\
\frac{1}{r^2} \frac{d}{dr} \left(r^2 \frac{d}{dr} \right) k + 2\Lambda k &= -\Lambda \\
+2\Lambda k &= -\Lambda \\
k &= -\frac{1}{2}.
\end{aligned} \tag{A.7}$$

We substitute the expression (A.6) into (A.1) to determine the required constant k . With respect to the theory of solving differential equations, the resulting solution will be given by the sum of the homogeneous part of the differential equation $\phi_0(r)$ and the particular solution $\phi_p(r)$. The overall vacuum analytical solution of (A.1) then follows

$$\phi_{vacuum}(r) = \phi_0(r) + \phi_p(r). \tag{A.8}$$

We verify our solution as

$$\begin{aligned}
& \frac{1}{r^2} \frac{d}{dr} \left(r^2 \frac{d}{dr} \right) \phi_p(r) + 2\Lambda \phi_p(r) = -\Lambda \\
& \frac{1}{r^2} \frac{d}{dr} \left(r^2 \frac{d}{dr} \right) \left(\frac{\bar{A}}{r} \cos(\sqrt{2\Lambda}r) + \frac{\bar{C}}{r} \sin(\sqrt{2\Lambda}r) - \frac{1}{2} \right) + \\
& \quad + 2\Lambda \left(\frac{\bar{A}}{r} \cos(\sqrt{2\Lambda}r) + \frac{\bar{C}}{r} \sin(\sqrt{2\Lambda}r) - \frac{1}{2} \right) = -\Lambda \\
& \frac{1}{r^2} \frac{d}{dr} \left(r^2 \left[\frac{-\bar{A}\sqrt{2\Lambda} \sin(\sqrt{2\Lambda}r)r - \bar{A} \cos(\sqrt{2\Lambda}r)}{r^2} \right] \right) + \\
& \quad + \frac{1}{r^2} \frac{d}{dr} \left(r^2 \left[\frac{\bar{C}\sqrt{2\Lambda} \cos(\sqrt{2\Lambda}r)r - \bar{C} \sin(\sqrt{2\Lambda}r)}{r^2} \right] \right) + \\
& \quad + 2\Lambda \left(\frac{\bar{A}}{r} \cos(\sqrt{2\Lambda}r) + \frac{\bar{C}}{r} \sin(\sqrt{2\Lambda}r) - \frac{1}{2} \right) = -\Lambda \\
& \frac{1}{r^2} \left(-\bar{A}2\Lambda \cos(\sqrt{2\Lambda}r)r - \bar{A}\sqrt{2\Lambda} \sin(\sqrt{2\Lambda}r) + \bar{A}\sqrt{2\Lambda} \sin(\sqrt{2\Lambda}r) - \right. \\
& \quad \left. - \bar{C}2\Lambda \sin(\sqrt{2\Lambda}r)r + \bar{C}\sqrt{2\Lambda} \cos(\sqrt{2\Lambda}r) - \bar{C}\sqrt{2\Lambda} \cos(\sqrt{2\Lambda}r) + \right. \\
& \quad \left. + 2\Lambda \left(\frac{\bar{A}}{r} \cos(\sqrt{2\Lambda}r) + \frac{\bar{C}}{r} \sin(\sqrt{2\Lambda}r) - \frac{1}{2} \right) = -\Lambda \right. \\
& \quad \left. - \frac{\bar{A}2\Lambda}{r} \cos(\sqrt{2\Lambda}r) - \frac{\bar{C}2\Lambda}{r} \sin(\sqrt{2\Lambda}r) + \right. \\
& \quad \left. + 2\Lambda \left(\frac{\bar{A}}{r} \cos(\sqrt{2\Lambda}r) + \frac{\bar{C}}{r} \sin(\sqrt{2\Lambda}r) - \frac{1}{2} \right) = -\Lambda \right. \\
& \quad \left. \left(-\bar{A}2\Lambda + 2\Lambda\bar{A} \right) \frac{\cos(\sqrt{2\Lambda}r)}{r} + \left(-\bar{C}2\Lambda + 2\Lambda\bar{C} \right) \frac{\sin(\sqrt{2\Lambda}r)}{r} + 2\Lambda \left(-\frac{1}{2} \right) = -\Lambda \right. \\
& \quad \left. -\Lambda = -\Lambda. \right. \\
& \quad \left. 0 = 0 \right. \\
& \quad \quad \quad (A.9)
\end{aligned}$$

The analytical solution of equation (A.1) in spherical symmetry for the vacuum given by (A.8) reads as

$$\phi_{vacuum}(r) = \frac{\bar{A}}{r} \cos\sqrt{2\Lambda}r + \frac{\bar{C}}{r} \sin\sqrt{2\Lambda}r - \frac{1}{2}. \quad (A.10)$$

A.2 Taylor series of the vacuum solution

Given the analytical solution (A.10), we write the Taylor series for $\sin(x)$ and $\cos(x)$ as

$$\sin(x) = \sum_{n=0}^{\infty} (-1)^n \frac{x^{2n+1}}{(2n+1)!}, \quad x \in (-\infty, +\infty) \quad (\text{A.11})$$

and

$$\cos(x) = \sum_{n=0}^{\infty} (-1)^n \frac{x^{2n}}{(2n)!}, \quad x \in (-\infty, +\infty). \quad (\text{A.12})$$

Let's write the first three terms of the series for (A.11) and (A.12)

$$\sin(x) \approx x - \frac{x^3}{3!} + \frac{x^5}{5!} - \mathcal{O}(x^7) \quad (\text{A.13})$$

and

$$\cos(x) \approx 1 - \frac{x^2}{2!} + \frac{x^4}{4!} - \mathcal{O}(x^6). \quad (\text{A.14})$$

Let's rewrite the vacuum analytical solution (A.10) as

$$\phi_{vacuum}(r) = \frac{1}{r} \left(\bar{A} \cos \sqrt{2\Lambda} r + \bar{C} \sin \sqrt{2\Lambda} r \right) - \frac{1}{2}. \quad (\text{A.15})$$

Substituting the series for (A.11) and (A.12) into (A.15) and we obtain

$$\begin{aligned} \phi_{vacuum}(r) \approx & \frac{1}{r} \left[\bar{A} \left[1 - \frac{(\sqrt{2\Lambda} r)^2}{2!} + \frac{(\sqrt{2\Lambda} r)^4}{4!} - \mathcal{O}((\sqrt{2\Lambda} r)^6) \right] + \right. \\ & \left. + \bar{C} \left[(\sqrt{2\Lambda} r) - \frac{(\sqrt{2\Lambda} r)^3}{3!} + \frac{(\sqrt{2\Lambda} r)^5}{5!} - \mathcal{O}((\sqrt{2\Lambda} r)^7) \right] \right] - \frac{1}{2}. \end{aligned} \quad (\text{A.16})$$

The vacuum solution of the Poisson equation in spherical symmetry is

$$\phi_{Poisson}(r) = \frac{D}{r}, \quad (\text{A.17})$$

where the sign is hidden in the constant D and due to the zero character of the Newtonian potential for $r \rightarrow \infty$ we set the other integration constant equal to zero.

The calculations are performed on the spatial scales of the galaxy. Due to the large variability of sizes, we chose our galaxy as a reference, i.e. spatial scales of the order of $\sim 10^{23}$ cm. For such scales, it is reasonable to consider the development of goniometric functions up to the cube at most, as each additional power represents an error below double precision levels, because $\Lambda \sim 10^{-56} \text{ cm}^{-2}$. We modify the expression for $\phi_{vacuum}(r)$ as

$$\phi_{vacuum}(r) \approx \frac{1}{r} \left(\bar{A} + \bar{C}(\sqrt{2\Lambda} r) - \bar{A} \frac{(\sqrt{2\Lambda} r)^2}{2!} - \bar{C} \frac{(\sqrt{2\Lambda} r)^3}{3!} \right) - \frac{1}{2}. \quad (\text{A.18})$$

We do not consider the displacement of the perturbed vacuum potential, so let's neglect the term $-\frac{1}{2}$, and also after a suitable normalization of the constants \bar{A} and \bar{C} we can observe the difference between the potentials for the vacuum case at the following level

$$\bar{C}(\sqrt{2\Lambda} r) - \bar{A} \frac{(\sqrt{2\Lambda} r)^2}{2!} - \bar{C} \frac{(\sqrt{2\Lambda} r)^3}{3!}. \quad (\text{A.19})$$